A PHOTOELASTIC STUDY OF THE STRESS DISTRIBUTION IN FLAT PLATE PANELS SIMULATING SHIP BULKHEADS

E. A. MILLER

J. T. METCALF, JR.

A PHOTOELASTIC STUDY OF THE STRESS DISTRIBUTION IN FLAT PLATE PANELS SIMULATING SHIP BULKHEADS

by

EDMUND ANDERSON MILLER

and

JOHN TRUMBULL METCALF, JR.

SUBMITTED IN PARTIAL FULFILLMENT OF THE
REQUIREMENTS FOR THE DEGREE OF
NAVAL ENGINEER

at the

MASSACHUSETTS INSTITUTE OF TECHNOLOGY

May, 1957

Thesis
M5859

A PHOTOELASTIC STUDY OF THE STRESS DISTRIBUTION IN FLAT PLATE PANELS SIMULATING SHIP BULKHEADS

by

EDMUND ANDERSON MILLER

and

JOHN TRUMBULL METCALF, JR.

SUBMITTED IN PARTIAL FULFILLMENT OF THE

REQUIREMENTS FOR THE DEGREE OF

NAVAL ENGINEER

at the

MASSACHUSETTS INSTITUTE OF TECHNOLOGY

May, 1957

A PHOTOELASTIC STUDY OF THE STRESS DISTRIBUTION IN FLAT PLATE PANELS SIMULATING SHIP BULKHEADS

by

EDMUND ANDERSON MILLER

and

JOHN TRUMBULL METCALF, JR.

Submitted to the Department of Naval Architecture and Marine Engineering on 20 May 1957 in partial fulfillment of the requirements for the degree of Naval Engineer.

ABSTRACT

This thesis is a continuation of the work started by Rockwell Holman, reference 1, and continued by references 2 and 3. The general objective is the collection and analysis of data which may be used to improve the design of ship transverse bulkheads. This thesis investigated the behavior of plates of aspect ratio 2:1, 3:1 and 5:1, subjected to a uniformly distributed load along the top edge, clamped at the ends, and either unsupported or rigidly supported along the bottom edge. The effect of stiffeners at the vertical centerline was investigated for all aspect ratios, and the effect of stiffeners at the centerline and quarter points was investigated for aspect ratio 3:1 only.

The photoelastic technique of investigation was used, and the distribution of vertical shear stress intensity was calculated along the clamped ends.

Duplicate models for all aspect ratios were manufactured both of Catalin 61-893, and Plexiglass. The Catalin models were used to determine the fringe pattern which was recorded photographically, and the Plexiglass models were used to determine the isoclinic patterns.

The vertical shear stress distribution along the clamped ends was obtained for all conditions, and these curves were plotted to show the effect of aspect ratio on this distribution for the various conditions of support. The effect of one stiffener on the shear distribution is shown. The effect of adding stiffeners at the quarter points of the 3:1 aspect ratio model was determined, as well as the effect of bottom support on the shear distribution for both stiffened and unstiffened plates.

The overall accuracy was determined to be within 15%.

Thesis Supervisor: Amelio M. D'Arcangelo

Title: Assistant Professor of Naval Architecture

ACKNOWLEDGEMENT

We wish to express our deep appreciation to the following:

Professor Amelio M. D'Arcangelo, of the Department of Naval Architecture and Marine Engineering, who acted as Thesis Supervisor for his assistance and encouragement during the preparation of this thesis.

Professor William M. Murray, of the Department of Mechanical Engineering, for his permission to use the facilities of the Stress Analysis Laboratory and whose aid and assistance were invaluable.

Professor J. Harvey Evans, of the Department of Naval Architecture and Marine Engineering, who assisted in formulating the basic program of this research and who through his efforts enabled us to obtain the special equipment needed in the experimental work.

Cambridge 39, Massachusetts
May 20, 1957

Secretary of the Faculty
Massachusetts Institute of Technology
Cambridge 39, Massachusetts

Dear Sir:

In accordance with the requirements for the Degree of Naval Engineer, we herewith submit a thesis entitled: "A Photoelastic Study of the Stress Distribution in Flat Plate Panels Simulating Ship Bulkheads."

Respectfully submitted,

Edmund Anderson Miller
Lieutenant, United States Navy

John Trumbull Metcalf, Jr.
Lieutenant, United States Navy

TABLE OF CONTENTS

		Page
	Title Page	i
	Abstract	ii
	Acknowledgement	iii
	Letter of Transmittal	iv
	Table of Contents	v
	Table of Illustrations	vi
	Tables of Data	viii
	Notation	ix
I.	Introduction	1
II.	Procedure	4
III.	Results	21
IV.	Discussion of Results	29
V.	Conclusions	33
VI.	Recommendations	35
VII.	Appendix	36
	A. Supplementary Introduction	37
	B. Details of Method and Procedure	41
	C. Calibration	47
	D. Original Data and Calculations	55
	E. Literature Citations	88

TABLE OF ILLUSTRATIONS

Figure I	Picture of the Polariscope and Laboratory
Figure II	Picture of the Polariscope and Laboratory
Figure III	Diagrammatic Sketch of the Polariscope set up as a Circular Polariscope with Dark Field
Figure IV	Picture of the Straining Frame Used
Figure V	Picture of the Uniform Loading Device
Figure VI	Plans and Dimensions of the Uniform Loading Device
Figure VII	Plot of τ_{xy} over the Clamped Edges for the Three Aspect Ratios, Unstiffened and Unsupported
Figure VIII	Plot of τ_{xy} over the Clamped Edge for the Three Aspect Ratios, Unstiffened and Supported
Figure IX	Plot of τ_{xy} over the Clamped Edges for the Three Aspect Ratios, Stiffened and Unsupported
Figure X	Plot of τ_{xy} over the Clamped Edge for the Three Aspect Ratios, Stiffened and Supported
Figure XI	Plot of τ_{xy} over the Clamped Edge for Aspect Ratios 3:1 with bottom unsupported for the three conditions of stiffening.
Figure XII	Plot of τ_{xy} over the Clamped Edge for Aspect Ratio 3:1 with bottom rigidly supported for the three conditions of stiffening.
Figure XIII	Plots of the Percentage Reduction in τ_{xy} max due to Addition of Bottom Support
Figure XIV	Calibration of Material
Figure XV	Calibration of Uniform Loading Device
Figure XVI	Presentation of Data and Isoclinics for A/R 5:1, Unstiffened and Unsupported
Figure XVII	Fringe Pattern for Figure XVI
Figure XVIII	Presentation of Data and Isoclinics for A/R 5:1, Unstiffened and Supported
Figure XIX	Fringe Pattern for Figure XVIII
Figure XX	Presentation of Data and Isoclinics for A/R 5:1, Stiffened and Unsupported

Figure XXI Fringe Pattern for Figure XX

Figure XXII Presentation of Data and Isoclinics for A/R 5:1, Stiffened and Supported

Figure XXIII Fringe Pattern for Figure XXII

Figure XXIV Presentation of Data and Isoclinics for A/R 3:1, Unstiffened and Unsupported

Figure XXV Fringe Pattern for Figure XXIV

Figure XXVI Presentation of Data and Isoclinics for A/R 3:1, Unstiffened and Supported

Figure XXVII Fringe Pattern for Figure XXVI

Figure XXVIII Presentation of Data and Isoclinics for A/R 3:1, Stiffened and Unsupported

Figure XXIX Fringe Pattern for Figure XXVIII

Figure XXX Presentation of Data and Isoclinics for A/R 3:1, Stiffened and Bottom Supported

Figure XXXI Fringe Pattern for Figure XXX

Figure XXXII Presentation of Data and Isoclinics for A/R 3:1, 3 Stiffeners and Bottom Unsupported

Figure XXXIII Fringe Pattern for Figure XXXII

Figure XXXIV Presentation of Data and Isoclinics for A/R 3:1, 3 Stiffeners and Bottom Supported

Figure XXXV Fringe Pattern for Figure XXXIV

Figure XXXVI Presentation of Data for A/R 2:1, Unstiffened and Bottom Unsupported

Figure XXXVII Fringe Pattern for Figure XXXVI

Figure XXXVIII Presentation of Data for A/R 2:1, Unstiffened and Bottom Supported

Figure XXXIX Fringe Pattern for Figure XXXVIII

Figure XL Presentation of Data for A/R 2:1, Stiffened and Bottom Unsupported

Figure XLI Fringe Pattern for Figure XL

Figure XLII Presentation of Data for A/R 2:1, Stiffened and Bottom Supported

Figure XLIII Fringe Pattern for Figure XLII

TABLES OF DATA

Table I Determination of Fringe Constant

Table II Calibration of Uniform Load Device

Table III Aspect Ratio 5:1

a. Unstiffened, bottom unsupported
b. Unstiffened, bottom rigidly supported

Table IV Aspect Ratio 5:1

a. Stiffened, bottom unsupported
b. Stiffened, bottom rigidly supported

Table V Aspect Ratio 3:1

a. Unstiffened, bottom unsupported
b. Unstiffened, bottom rigidly supported

Table VI Aspect Ratio 3:1

a. Stiffened (centerline), bottom unsupported
b. Stiffened (centerline), bottom rigidly supported

Table VII Aspect Ratio 3:1

a. Stiffened (centerline and quarter points), bottom unsupported
b. Stiffened (centerline and quarter points), bottom rigidly supported

Table VIII Aspect Ratio 2:1

a. Unstiffened, bottom unsupported
b. Unstiffened, bottom rigidly supported

Table IX Aspect Ratio 2:1

a. Stiffened, bottom unsupported
b. Stiffened, bottom rigidly supported

NOTATIONS

σ_1, σ_2	Principal Stresses (pounds per square inch)
σ_x, σ_y	Stresses in x and y directions (pounds per square inch)
τ_{max}	Maximum Shear Stress at any point (pounds per square inch)
τ_{xy}	Shear Stress in the plane perpendicular to the x axis, and in the y direction, also called vertical shear stress (pounds per square inch)
f	Fringe Constant of the material used (Catalin 61-893) (pounds per inch-order)
h	Thickness of the model (inches)
n	Order of Interference
b	Depth of model in the y direction (inches)
l	Distance between model supports (inches)
M	Bending moment (pound - inches)
y	Distance from neutral axis to any point of the model (inches)
I	Moment of Inertia of any cross section (inches ^{4})
A/R	Aspect Ratio
Δ	Denotes a small change in the letter following
w	Uniform load (pounds per inch)

I INTRODUCTION

Structural design is at best an inexact science. It is based on the theory of elasticity; however, the idealized conditions assumed for the theory of elasticity are rarely met by the actual structure. Conditions of restraint and support, fabrication errors and dimentional tolerences, and residual and locked-in stresses, are but a few of the sources of error which are present in the actual structure, and which are not considered in the mathematical solution of the structural design problem. Therefore, the design engineer must have the best possible information as to the magnitude and distribution of the stresses within the structure, under given conditions of load and restraint in order to design it intelligently and efficiently.

The theory of elasticity gives mathematical solutions for many types of problems involving both simple beams and plates. Deep beams fall in the area between simple beams and plates, and mathematical solutions for these beams are cumbersome and time consuming, (ref. 8). Therefore, other means have been used to solve these problems, and it is the basic research in the field of experimental stress analysis that gives the engineer much of the information that he needs for structural design.

Model experiments are easily adapted to laboratory work, and extrapolation from model to full scale structure is possible without serious error, (ref. 5). A very popular technique for measuring stress within a model is the use of the polariscope, (ref. 5). The information obtained from the observation of a model in a polariscope is sufficient to calculate the magnitude and distribution of stress at all points within the model. This then serves as a basis for developing design techniques, as well as a check on the accuracy of the assumptions made by the designer.

The transverse bulkheads of a ship in general fall into this nebulus area between simple beams and plates. Design criteria have been evolved and used successfully for many years. Current practice in bulkhead design as specified by the Bureau of Ships is that "the vertical load which is considered to be distributed to the boundaries by shear, should be based upon a shear stress in the plating for one deck height (or where no deck is connected below the point of application of the load, then seven feet) of about one half of the critical shear stress for the thickness of plating and the size of the panel in question," (ref. 2). An attempt to substantiate this design criterion was initiated at Massachusetts Institute of Technology by reference 1 and continued in reference 2 and reference 3. This thesis is intended to be a contribution to this long term goal.

The analytical solution to the stress distribution in a deep beam with clamped ends has never been presented, and the first photoelastic analysis of the problem were presented in references 1, 2, and 3. The investigations to date have been confined to deep beams of varying aspect ratios, clamped ends, and subjected to a point load. This thesis investigates the behavior of similar beams under a uniformly distributed load, and to the writers' knowledge, is the first photoelastic investigation of this problem.

Several methods of applying a uniform load have been devised for laboratory use. The method used for this thesis is adapted from reference 4, using hydraulic pressure within a gum rubber tube to apply the load uniformly along the top edge of the plate. Models of aspect ratio 2:1, 3:1, and 5:1, were investigated under the following conditions:

1. Plate unstiffened, ends clamped, bottom free.
2. Plate unstiffened, ends clamped, bottom rigidly supported.
3. Plate stiffened, ends clamped, bottom free.
4. Plate stiffened, ends clamped, bottom rigidly supported.

In addition, aspect ratio 3:1 was investigated with stiffeners on the centerline and at the quarter points under conditions 3 and 4 above.

It is believed that these conditions of load and restraint straddle the actual conditions that exist for a ship's transverse bulkhead. Therefore, once the stress magnitude and distribution are determined for points within the model, the results may be extrapolated to the full scale structure, and the bulkhead design criterion may be substantiated or refined, as determined by the findings of this series of experiments.

II PROCEDURE

1. Polariscope

The polariscope used for the experimental work envolved in this thesis is the polariscope located in the Ship's Structures Laboratory of the Department of Naval Architecture and Marine Engineering. This polariscope is Model No. 402, manufactured by the Polarizing Instrument Company of Irvington-on-the-Hudson, New York. The polariscope, together with the laboratory set up is shown in Figures I and II.

The polariscope may be divided into two parts, one on either side of the straining frame. The individual components of the polariscope are mounted on two optical benches consisting of two straight parallel steel tracks supported on legs. The bench carrying the light source is called the light source bench and the bench carrying the camera is called the camera bench. Reading from left to right in Figure I, the components mounted on the light source bench are the light source, a collimating lens, and the polarizer assembly. On the other side of the straining frame, the components mounted on the camera bench are the analyzer assembly, a second collimating lens, the camera lens, and the camera.

The light source may be used to supply either white light or mercury green light. The two lamps are mounted on a turn table inside the light source housing. This turn table may be rotated by means of a knurled disk in order to bring either of the lights into position. The white light is generated by an ordinary 300 watt incandescant lamp. The mercury green light is generated by a special mercury vapor lamp, Model XSAH 250-54 Westinghous Mercury Arc Lamp. This lamp generates a light which is very nearly a perfect monochromatic light allowing very precise definition in the isochromatic fringe pattern in areas of high stress variation.

Figure I

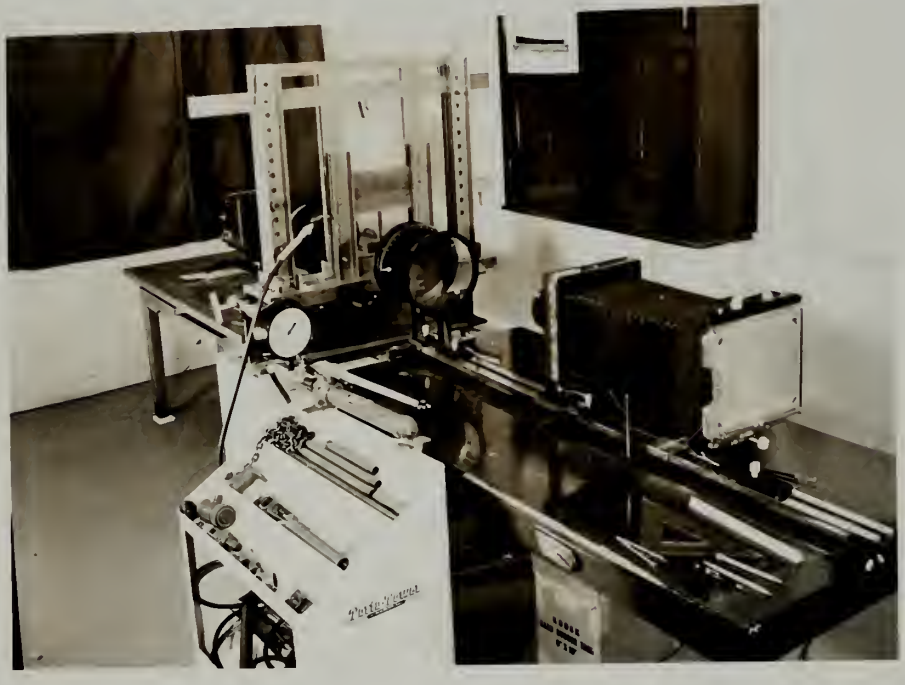

Figure II

Two independant switches on the outside of the light source housing allow the selection of either light. On the face of the housing is a masking plate with two small holes of different diameters, 1.5 mm and 3 mm diameters respectively. The masking plate is mounted on the housing by means of a pivot thereby allowing the operators to select either the 1.5 mm hole or the 3 mm hole as the aperture for transmission of the light through the system. Normally, the small hole is used with the mercury arc lamp when photographs are to be made and the large hole is used with white light when iso-clinic lines are to be traced.

Next to the light source in the path of light is located a collimating lens. The purpose of this lens is to convert the divergent light rays from the point source into parallel light rays. The lens is 8 1/2 inches in diameter and is fixed in a ring frame. This lens is positioned on the obtical bench in the following manner. The white light source is turned on and a mirror is placed at the end of the bench with the plane of the mirror perpendicular to the tracks. The lens is then mounted on the tracks and is moved laterally along the tracks until the reflected image of the light source from the mirror back onto the face of the light source housing is the same diameter as the aperture on the masking plate. When this position is found, both the light source housing and the collimating lens are firmly fixed to the bench by means of the locking screws.

Next to the collimating lens is located the polarizer and its quarter wave plate. Polarization is accomplished by using a polaroid disk 8 1/2 inches in diameter. Both of these plates are mounted in ring frames similar to that used for the collimating lens except that they may be rotated through a 180° angle independantly. A pointer is attached to each of the rotating plates. On the stationary ring frame is inscribed at one degree intervals an angular scale, reading from 0° at the horizontal to 90° at the vertical.

When the polarizer is set at 90°, the plane of the polarizing plate is vertical. The quarter wave plate is attached to the assembly frame on a friction pivot and may quickly be swung up into position to produce a circular polariscope or down out of the light path to produce a plane polariscope. The polarizer assembly is mounted on the tracks as close to the end of the bench as possible.

Next to the polarizer is the straining frame containing the model. This device is not part of the polariscope proper and is described in the next section.

Next to the model on the camera bench is the analyzer assembly. The analyzer assembly is identical to the polarizer assembly except that the quarter wave plate preceeds the polaroid disk and that the plane of transmission of the quarter wave plate and the polaroid disk are perpendicular to those in the polarizer assembly. When all plates are set at 90°, we have the normal circular polariscope with dark field as indicated in Figure III. The analyzer assembly is positioned on the tracks as close to the end of the tracks as possible.

Following the analyzer assembly is another collimating lens. This lens is identical to the preceeding collimating lens. Its function is to take the parallel light rays and focus them to a point so that the image of the model may be brought into the camera. This collimating lens is positioned on the tracks about 5 inches from the analyzer assembly. Its position in relation to the analyzer is not critical. When the analyzer and the collimating lens have been positioned, they are firmly locked to the tracks by means of the locking nuts.

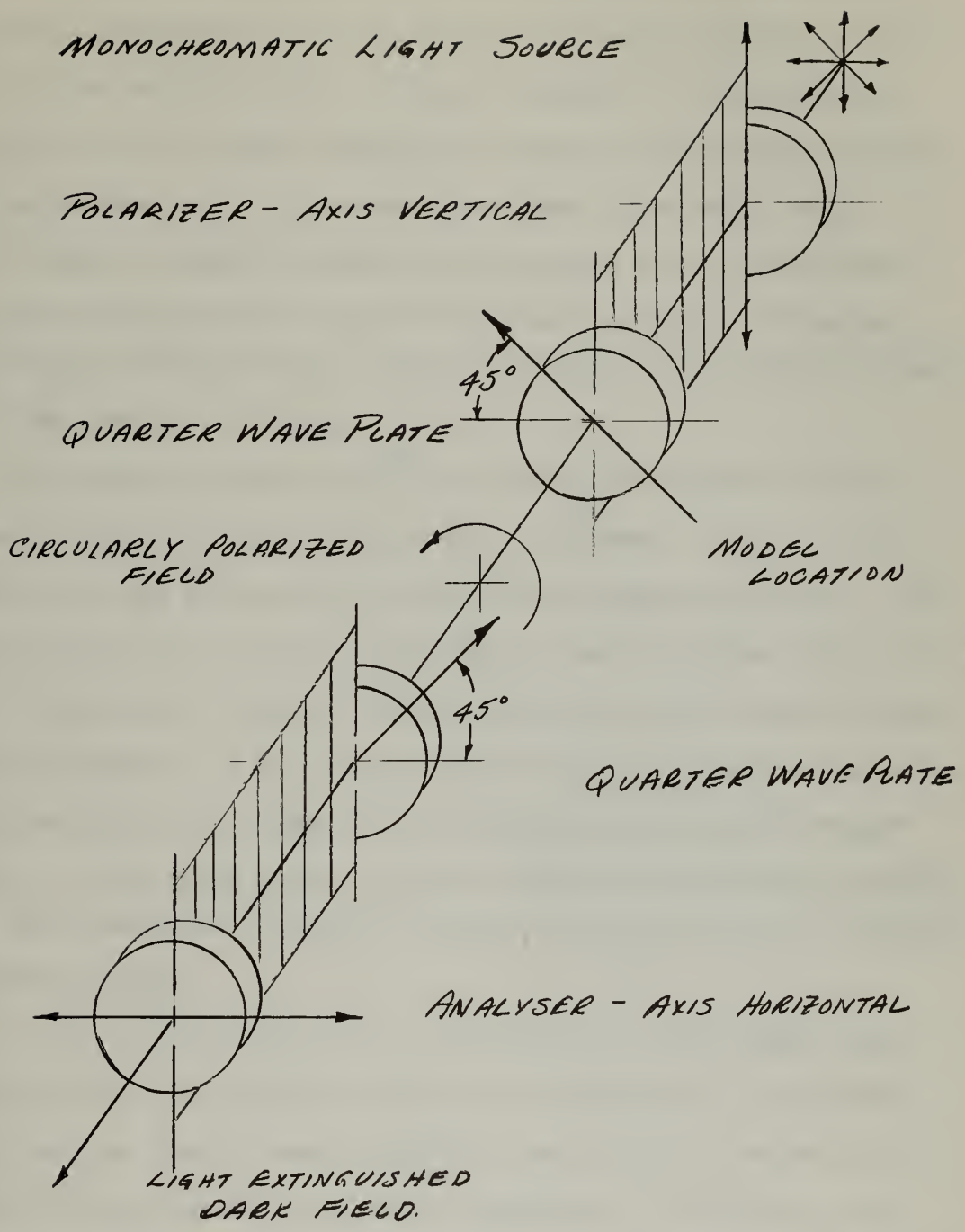

FIGURE III.

STANDARD OR CROSSED CIRCULAR POLARISCOPE

J.T.M.

Next on the tracks comes the camera lens. The camera lens is composed of the camera lens proper and a dark green filter (Wratten #77) attached to the lens by a friction sleeve. To remove the filter, hold the lens and twist the filter off. The lens is attached to its mounting frame on a rack and pinnion arrangement by means of which small adjustments may be made in the longitudinal position of the lens. White light is passed through the system and the camera lens is placed where the second collimating lens focuses the light to a point. If the two tracks are not exactly aligned, the point of light will not hit the camera lens in the center of the lens.

If the point of light does not hit the camera lens correctly then the two tracks must be aligned. This is done as follows: First the table on which the light source bench is placed must be made horizontal. The table is checked with a spirit level and the legs are shimmed until the table is horizontal. Next the table on which the camera bench is placed is made horizontal. If the light point hits the camera lens on the horizontal centerline of the lens it may be adjusted by moving the tracks slightly. If the light point is above or below the horizontal centerline, one of the tables must be raised or lowered to bring the point of light to the correct position.

The camera proper is placed so that the hood on the shutter board covers the lens. The forward locking nut is then secured. The ground glass screen may then be moved along the track until the desired size of the model on the ground glass screen is obtained. The position of the ground glass has nothing to do with the focus of the model image. If the polariscope is properly set up, the model image is in focus for all positions of the ground glass plate; therefore, the position of the ground glass has only to do with magnification. For the experiments in this thesis the ground glass was set to give 1 x 1 magnification.

The film in the camera is standard 8 x 10 cut film and a cut film holder is provided. Exposure speeds on the shutter vary from 1/2 second to 1/50 of a second with bulb and time exposure positions. The aperture in the shutter may be fully controlled from all the way open to shut.

In order to trace the isoclinics, a tracing table is provided which is interchangeable with the ground glass screen. The light is reflected up to a horizontal tracing glass by means of a mirror set at 45°. If a tracing is to be made at the same scale used for taking a photograph, the bellows must be readjusted in as much as the image is expanded because of the greater length of travel of the light rays.

2. The Straining Frame

The straining frame used in this thesis was designed as part of reference 1 and is pictured in Figure IV. In the original design, the load was applied by hanging a tank on a lever and filling the tank with water. In this thesis, no point loads were applied and the frame was used merely to clamp the model plate and hold it securely against the uniform loading device, designed to apply a uniform load across the top of the plate. This device is described in detail in the following section. As may be seen in Figure IV, the model and uniform loading device are clamped between two channel beams by means of steel bolts spaced at 7 7/8 inch intervals. In order that as much friction as possible be generated between the frame and the catalin models to assure good clamping of the edges of the model, 3/16 inch steel chocks were inserted on either side of the model between the model and the channels. Emery paper strips were then placed between each face of the faying surfaces and the bolts were drawn as tight as possible without having them shear. In several instances, the limit was exceeded and the bolts either sheared or the threads stripped. It is believed that good clamping was achieved; however, it is impossible to state with any degree of certainty just how much clamping was achieved and at just what point this clamping took place in the model. Evidence that good clamping was achieved may be seen in the isochromatic fringe patterns obtained and in the fact that when the load was removed, the model returned to its original stress free condition. It is not felt that the method used in this experiment is entirely satisfactory because of the limitations mentioned above and it is suggested that some improved method be devised.

FIGURE IV

FIGURE V

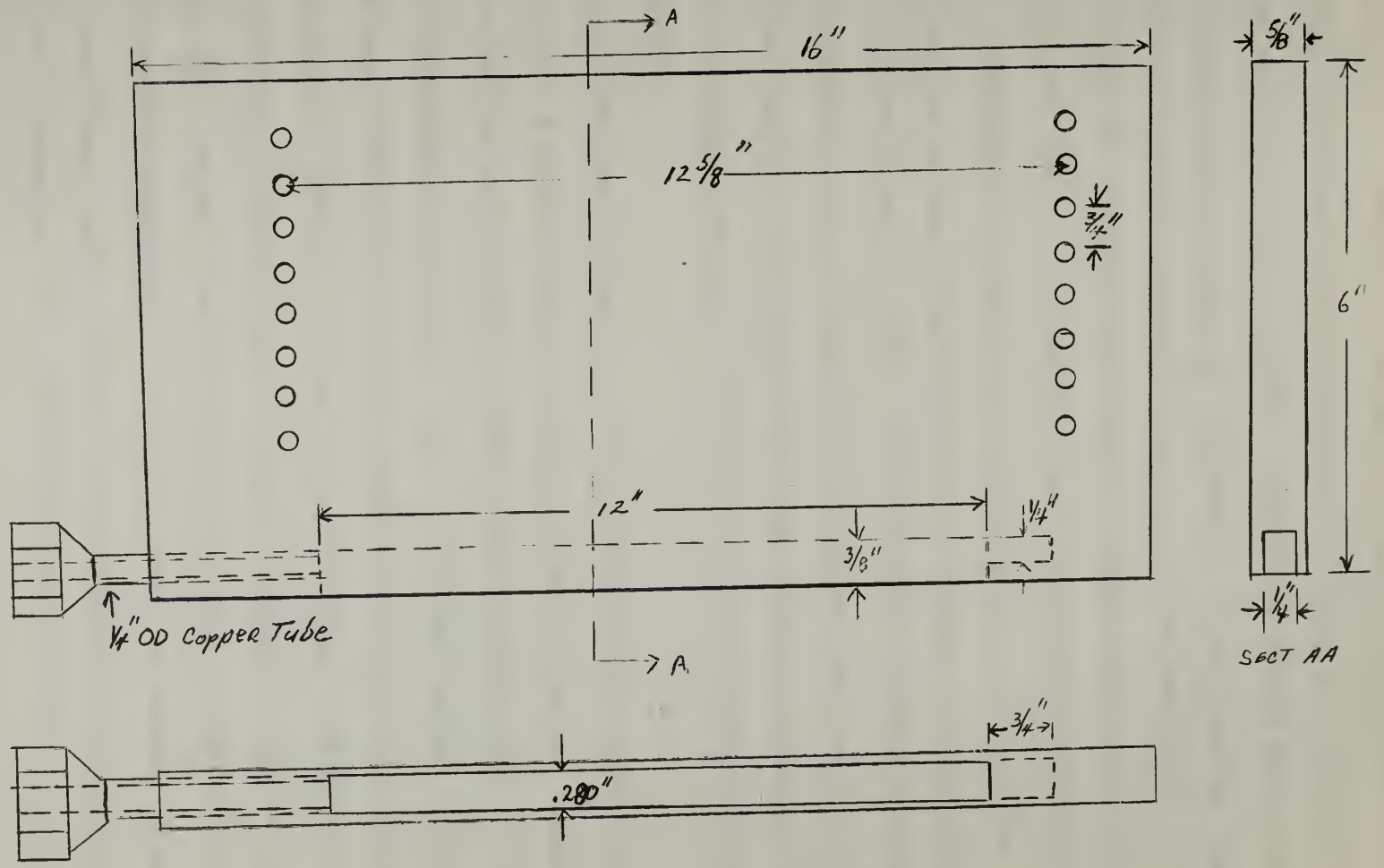

UNIFORM LOAD DEVICE
Figure VI

3. The Uniform Load Device

The basic idea involved in the uniform loading device used in the experiments in this thesis was obtained from reference 4. Applying the principles set forth in this reference, the uniform loading device with the necessary modifications to meet the requirements of this work was designed. This device is pictured in Figure V and the plans for this device are shown in Figure VI. Basically, this device is nothing more than a gum rubber tube contained in a rectangular slot with hydraulic pressure in the tube. The edge of the model to be tested is placed in the slot securely against the rubber tube and hydraulic pressure is applied by means of a portable hydraulic pump. The pressure is measured by means of a gage connected to the oil line. The load applied along the plate is a function of the pressure in the tube but this load cannot be calculated directly. In order to determine the load on the plate, the device must be calibrated experimentally.

Three independent methods were used to calibrate the device and determine whether or not a uniform load was applied. First, a plate of catalin was placed in the slot and rigidly supported along its bottom edge. No other restraint was applied to the model. This placed the specimen in pure compression. Theoretically, as the pressure in the tube was increased, the uniform load was increased. If the load was uniform, the plate as viewed in the polariscope should gradually change from opague or dark to translucent or light and the intensity of the light passed through the plate should be uniform throughout. The plate performed as expected except that an insufficient number of orders were observed to give any reliable calibration information. This test did serve to give evidence that the

applied load on the plate was uniform along the edge. Next, a catalin model 12 inches by 1.906 inches deep by .250 inches was simply supported on two points 11 inches apart. Once again, the pressure in the tube was raised and the fringe orders were counted as they passed a marked point on the plate 3/4 inches from the centroid of the plate. As each order passed the mark, the pressure indicated on the gage was recorded. The bending stress in the plate for each order was then calculated from photoelastic theory. From this stress, the geometry of the plate, and simple beam theory, the bending moment necessary to produce this stress was calculated, and finally from the bending moment the uniform load was calculated. The uniform load as calculated was then plotted versus gage pressure as shown in Figure XV. As a check on the above calculations, a Baldwin SR - 4 Load Cell was placed under one of the point supports and the load was again applied. The force as measured by the load cell was then used to calculate the uniform load by statics using the geometry of the plate and the supports. The two calibrations were compared and a difference of some 3% was found.

During the course of the experiments, certain modifications for improvement in the uniform loading device became apparant. Reference 4 suggested using an inert gas as the pressure medium. In as much as pressurized inert gas was not immediately available and the hydraulic equipment was, it was decided to use hydraulic oil as the pressure medium. It was realized that the oil would eventually cause the rubber to break down; however, it was felt that a tube would surely last for two or three weeks and this was all that was required. Such was not the case. Under the high pressure used to apply the load (500 psi), the rubber tubing deteriorated almost immediately and at the end of a day's work, the tubing would have become brittle and

weak. The high pressures and the oil combined to make the tube swell and seal itself off inside the copper tube. Because of this a new tube had to be inserted every day. In addition, the gum rubber tubing under the high pressures became very sensitive to any weak spots in the tube or rough places on the device causing a rupture in the tube. When this happened under high hydraulic pressure, oil was sprayed over the equipment causing a disagreeable mess. Gas would be much cleaner than oil. Another disadvantage with using oil is the necessity of bleeding air from the tube and replacing the air with oil. While this is not particularly difficult, it is time consuming. Finally, the pressure in the system while under test tends to vary. The valves in the pump will not hold the pressure steady. An additional choke valve was installed in the line but even this would not hold the pressure steady at the higher pressures. Small leaks in the oil line and small leaks through the valves tended to bleed this pressure off. Pressurized gas operating through a reducing valve would correct all of the above mentioned defects.

During the course of the experiments, there was doubt at times as to the exact pressure in the tube. This was caused by the tendency of the tube to swell and seal itself off. Two modifications would correct this defect. First, an additional gage should be installed on the opposite side of the loading device from the pump. With two pressure gages reading the same pressure on opposite sides of the model, the pressure inside the tube would be known with certainty. Secondly, the diameter of the copper tube used to attach the hydraulic fitting to the plate should be changed so that the inside diameter of the copper tube is the same diameter as the outside diameter of the gum rubber tube. It was originally felt that the copper tube and the gum rubber tube should have the same outside diameters

and a pure gum rubber tube with an 1/8 inch ID and 1/16" wall thickness was selected in order to insure a seal for the hydraulic oil. The only seal between the copper tube and the gum rubber tube is the rubber on the copper acting in conjunction with the pressure inside the tube. The rubber tube is placed inside the copper tube by serving one end of the rubber and stretching it out until it would pass through the copper tube. After the rubber tube had been pulled through the copper tube, it was merely clipped off and allowed to snap back. No further attempt was made to form a seal. This action tended to reduce the inside diameter of the rubber tube to approximately 1/32 of an inch. As the tube swelled under pressure, this small opening was closed off. There was no tendency at all for the oil to leak between the rubber and the copper even at the highest pressures, and since the tube almost doubles its diameter after it has been subjected to high pressure, it may reasonably be assumed that this modification would also be leakproof.

The placing of an additional gage on the opposite side of the device from the pump would give an additional advantage. In the present device the rubber tube must be sealed at its bitter end. This is done by cutting a piece of the tube about an inch long and placing this over the pressure tube at the bitter end to form a cushion for the pressure tube. The tube is then sealed by putting a drop of rubber cement inside the pressure tube and serving the end of the tube as tightly as possible using fine copper wire. This has a tendency to pinch the pressure tube even with the additional layer of rubber acting as a cushion. This spot where the end of the tube is served is the weakest spot in the device. Out of approximately 12 failures experienced all except three occured at this spot. Two failures occured at the other end of the slot where the rubber tube leaves the copper tube

and the other failure occured at midlength of the test model and was apparantly caused by a fault in the gum rubber tubing. If an additional gage were installed, the gum rubber would merely be fed through the copper tube and allowed to snap back just as on the pump side.

The critical dimensions on the uniform loading device are the dimensions of the slot. The dimensions of the steel plate were selected so that any deflection of the steel plate would be less than 1/100 th of the deflection of the test models and so that the plate would fit comfortably in the straining frame. A slot 12 inches long was chosen because the catalin material from which the models were made is supplied in plates approximately 12 inches long and it was thought that models as large as possible should be tested. This was a mistake. The models and consequently the slot should have been made only 6 inches long. This would have permitted the entire model to be photographed in the polariscope under strain instead of only half of the model, it would have permitted the investigation to be extended to an Aspect Ratio of 1:1, and it would have saved immeasurable time in preparing the models. The depth of the slot should be 1 1/2 times the diameter of the gum rubber tube to be used, and the clearance of the slot between the model and the steel should be at least .005 inches per side but should not exceed .015 inches per side. To have a clearance smaller than .005 inches would give difficulty in placing the model in the slot and might tend to introduce some friction between the plate and the device. To exceed .015 inches clearance is to invite the tube to blow out under high pressure. To minimize the danger of the latter happening and to offer some protection to the gum rubber tube, a rubber strip was placed over the tube between the tube and the model. This strip saved a rupture on several occasions. The strip is merely a piece of electric insulation tape without adhesive.

4. Model Preparation

The models used in this thesis to obtain the isochromatic fringe patterns were made of Catalin 61-893 (formerly Bakelite 61-893). This material comes from the manufacturer in sheets approximately 6 x 12 inches in varying thicknesses up to 1 inch. The material used in this thesis was a nominal 1/4 inch sheet. In its rough state, the material has been cast and the surfaces have been ground. To prepare a stress free model, the material must be annealed and polished. The material is annealed by placing it in an oil bath on a piece of flat glass and raising the temperature of the oil bath to about 250°F in an oven. The material is allowed to soak at this temperature for about 8 hours and then the temperature is gradually lowered in steps during a 24-hour period. After this treatment, the material should be stored for approximately one month before using. In its cast and annealed state, the material is only roughly dimensioned. It may vary in thickness by as much as 1/32 inch and in its long dimensions by as much as 3/4 inch.

To polish the material, one starts by sandpapering the material until the plate is within about .020 inches of the desired thickness. The surfaces are then ground 'true' on a flat cast iron lap using a carborundum grit of about 220. When the surfaces are true, the size of the grit is gradually reduced until a #600 grit is reached. All of these abrasives are suspended in water and the water is liberally applied. After the plate has been ground with #600 abrasive, the plate is switched to a lap covered with velvet or canvas and is polished with levicated aluminum oxide until a high gloss is obtained and no noticeable scratches are present. Minor scratches may be covered up by applying a thin coat of light mineral oil to the plate such as Nujol and then carefully wiping the plate until all smears are removed.

The above process is a most tedious and time consuming one. It is also most difficult to accomplish because if one speck of grit gets onto the lap or if the lap is not perfectly smooth when grinding the plate with the #600 grit, deep scratches will be cut into the plate making it almost impossible to polish. This part of this thesis was the most time consuming part of the work and little of value was gained. The Catalin Corporation will furnish the material already annealed and polished at extra charge. It is strongly recommended that any future work with Catalin that the material be ordered from the manufacturer already annealed and polished. In addition, there is a material known as CR 39 furnished by Chapman Laboratories, West Chester, Pennsylvania, which is claimed by the manufacturer to need no annealing or polishing and is said to free of time edge effects. It is suggested that this material might be tried. Catalin is seriously affected by time edge effects which begin to form within 48 hours after the edges are milled.

After the plates have been polished, the outline of the model to be made is scratched lightly on the plate with a sharp tool. The plate is then rough cut to dimensions using a hack saw or a power metal saw. A saw intended to use on wood is not satisfactory. The final cut to size is made using a high speed vertical mill and a template. The final cut should not exceed .005 inches and the material should not be forced. If it is overheated, stresses will be introduced into the model. For the plates used in this thesis, a reference grid of one-inch squares was lightly scratched on one side of the model.

III RESULTS

1. Isochromatic fringe patterns for the fourteen conditions investigated are shown in Figures XVII, XIX, XXI, XXIII, XXV, XXVII, XXIX, XXXI, XXXIII, XXXV, XXXVII, XXXIX, XLI, and XLIII.
2. Isoclinic patterns for ten conditions and plots of vertical shear distribution for all fourteen conditions are shown in Figures XVI, XVIII, XX, XXII, XXIV, XXVI, XXVIII, XXX, XXXII, and XXXIV, XXXVI, XXXVIII, XL, XLII.
3. The effect of aspect ratio on vertical shear stress intensity in unstiffened, unsupported plates with clamped ends is shown in Figure VII.
4. The effect of aspect ratio on vertical shear stress intensity in unstiffened, rigidly supported plates with clamped ends is shown in Figure VIII.
5. The effect of aspect ratio on vertical shear stress intensity in stiffened, unsupported plates with clamped ends is shown in Figure IX.
6. The effect of aspect ratio on vertical shear stress intensity in stiffened, rigidly supported plates with clamped ends is shown in Figure X.
7. The effect of the number of stiffeners on the vertical shear distribution in plates of aspect ratio 3:1 with bottom unsupported and ends clamped is shown in Figure XI.
8. The effect of the number of stiffeners on the vertical shear distribution in plates of aspect ratio 3:1 with bottom rigidly supported and ends clamped is shown in Figure XII.
9. The effect of bottom support on maximum vertical shear stress intensity is shown in Figure XIII, for both unstiffened and stiffened plates.
10. The accuracy of these experiments was determined to be within 15%. This was calculated by comparing the total load on the top of the plate to twice the integral of the vertical shear stress intensity along the clamped end of the plate multiplied by the thickness of the plate with the plate in the unsupported condition.

Figure VII

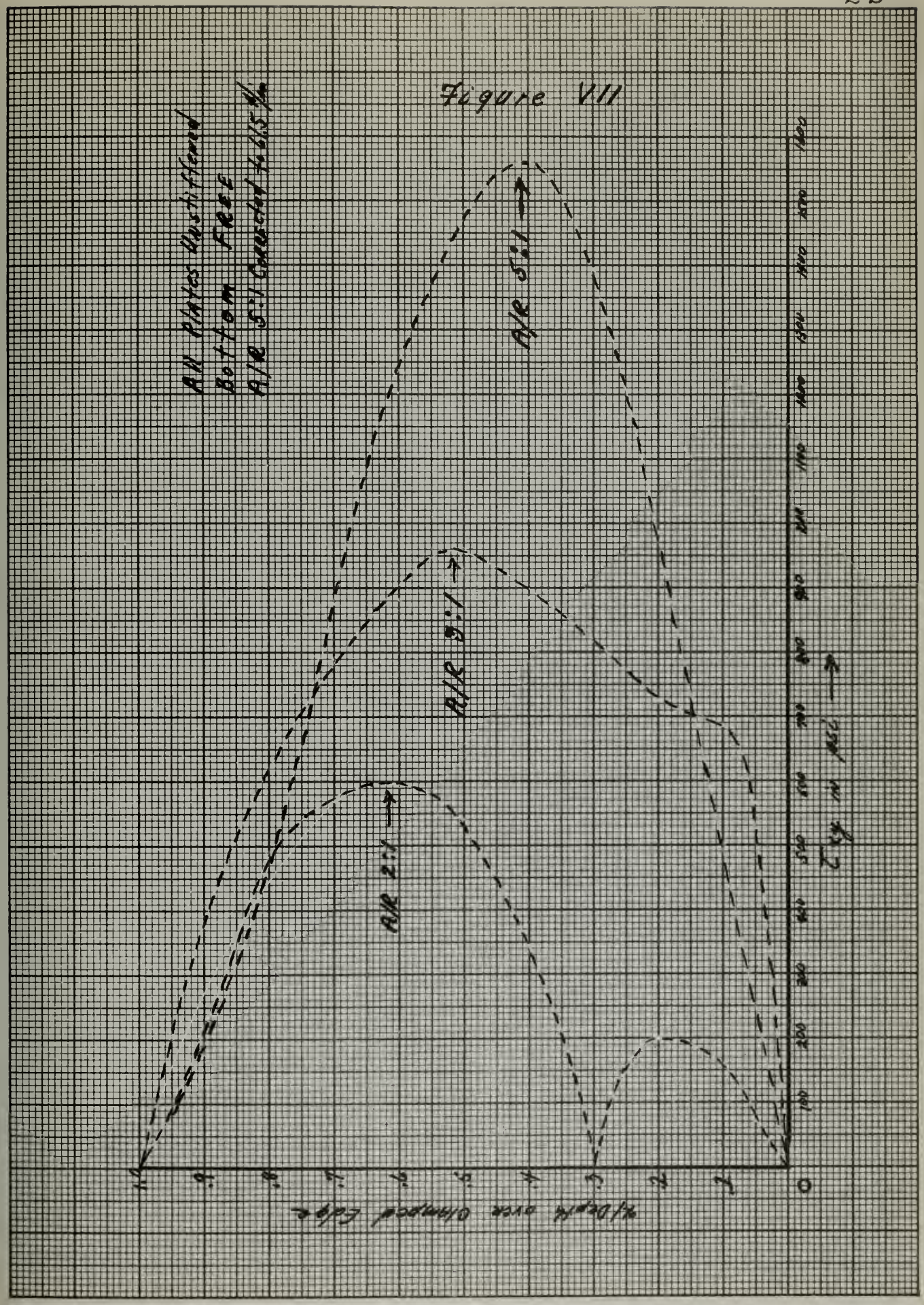
All plates unstiffened
Bottom free
A/R 5:1 Corrected for ϕ=45°
A/R 5:1
A/R 3:1
A/R 2:1
% Deflection over diameter each
Load per sq. in.

Figure VIII

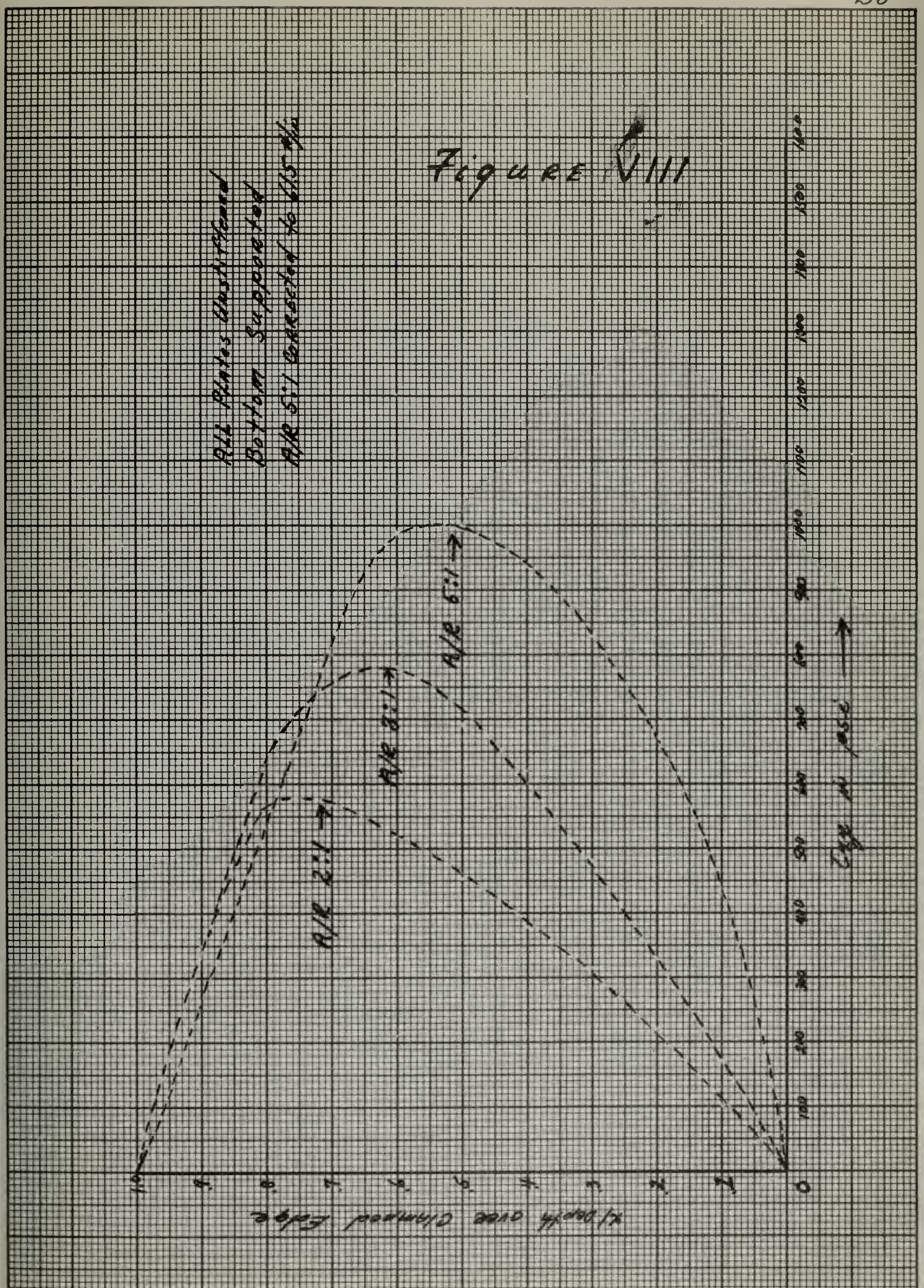
Bottom Superimposed Pressure Distribution
with Basic Unsymmetrical Airfoil
Re 5.1 Million
x/ Depth over Chamber Line
Pressure Coefficient
R/R 12:1
R/R 9:1
R/R 6:1

FIGURE IX

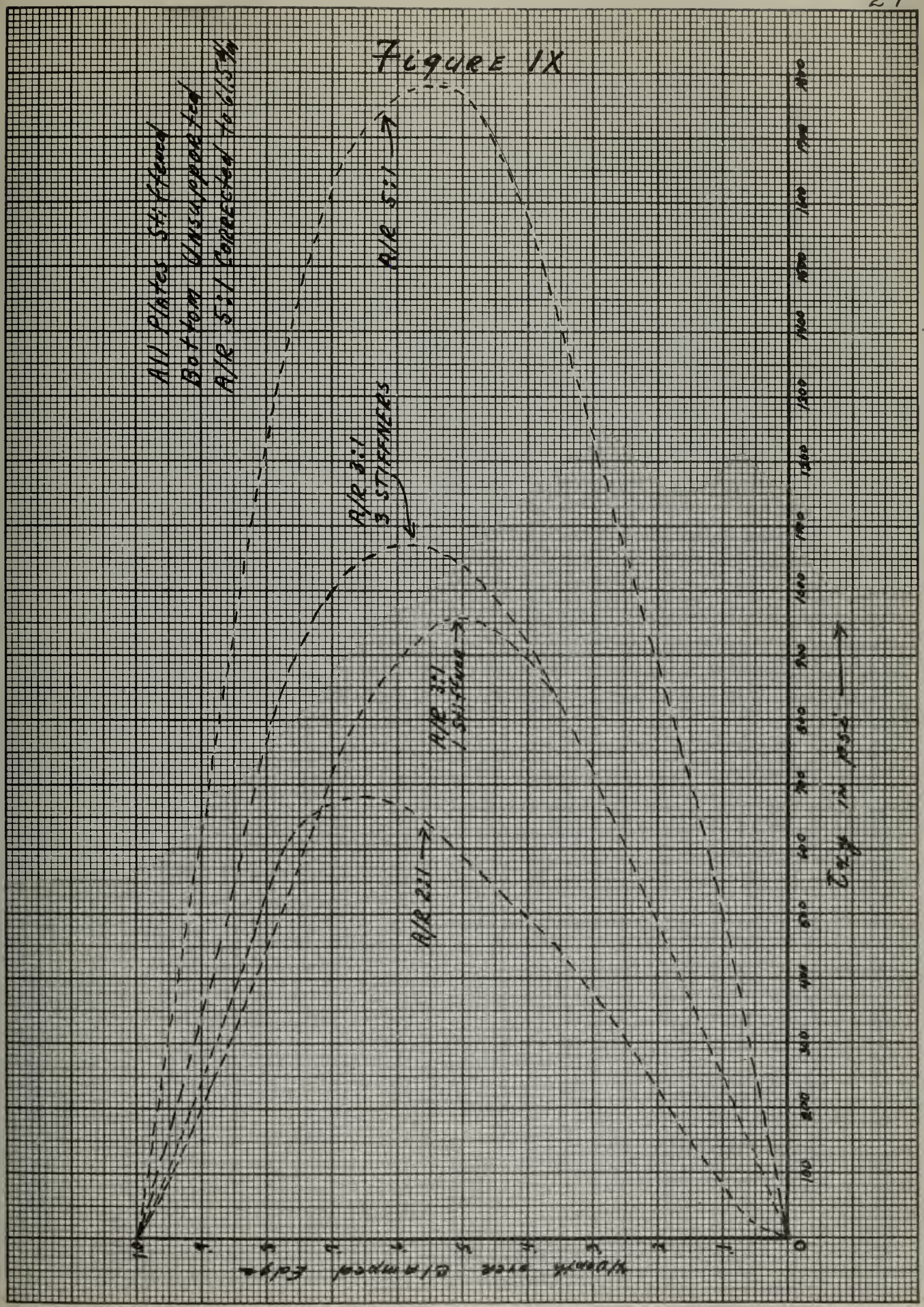
All Plates Stiffened
Bottom Unstiffened
A/E 3:1 Connected Flanges
A/E 5:1
A/E 3:1
3 STIFFENERS
A/E 3:1
A/E 2:1
Load per Inch
Width over Flanged Edge

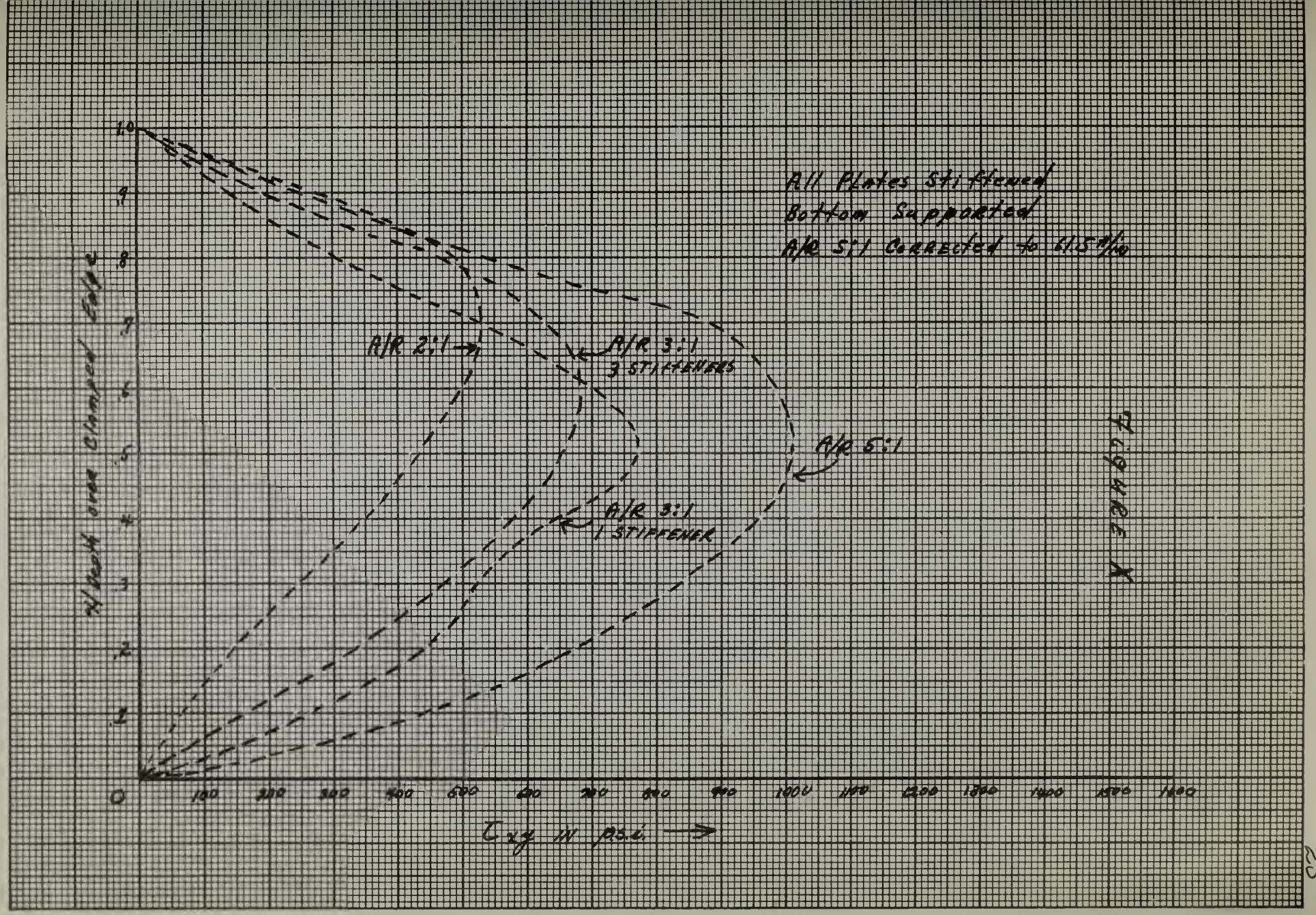
All Plates Stiffened
Bottom Supported
A/R 5:1 Corrected to 6.15 %
A/R 2:1
A/R 3:1
3 STIFFENERS
A/R 5:1
A/R 3:1
1 STIFFENER
Figure X
% Area Change Edge
10
9
8
7
6
5
4
3
2
1
0
100
200
300
400
600
800
1000
1200
1400
1500
1600
Σxy in psi.

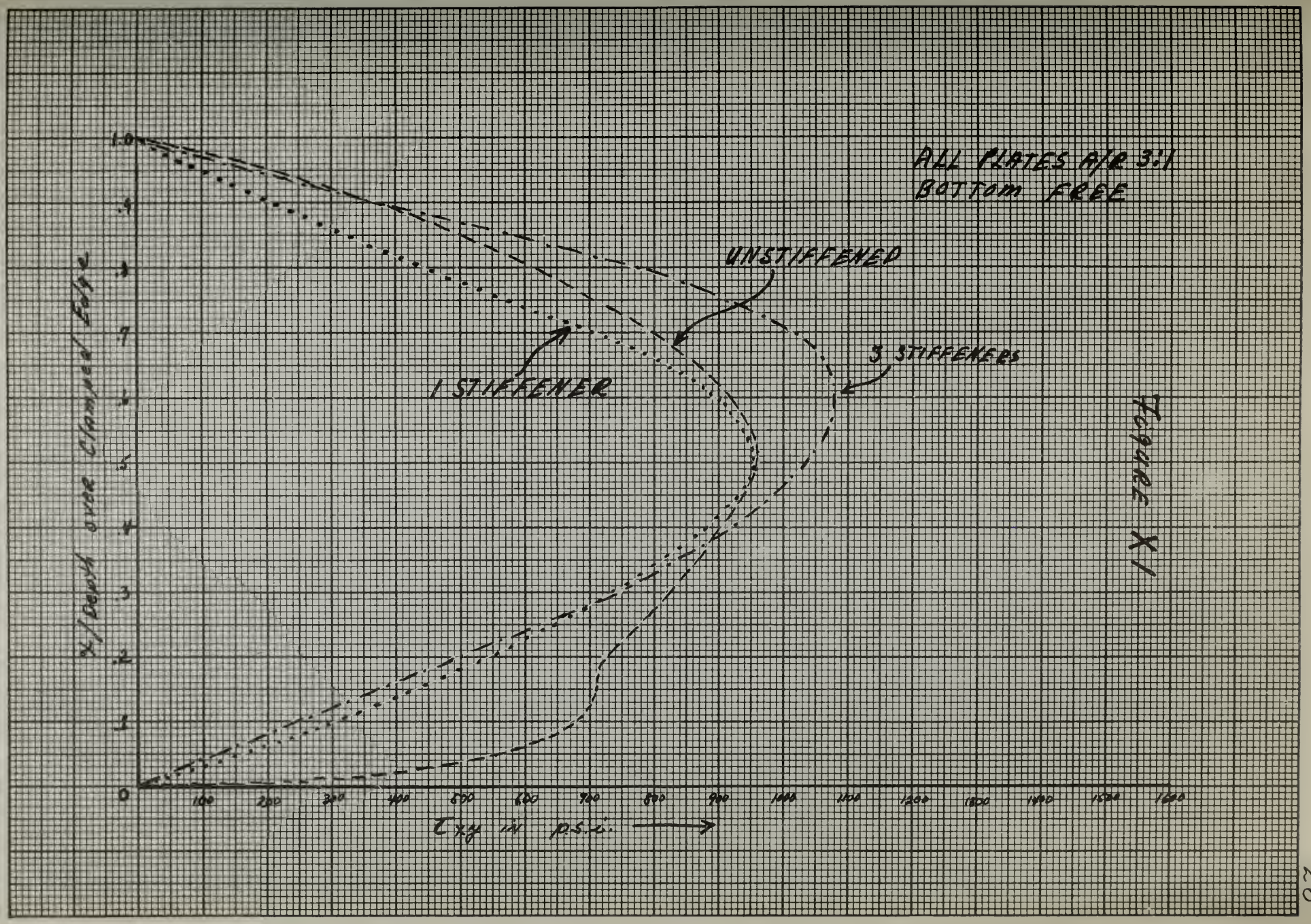
ALL PLATES A/B 3:1
BOTTOM FREE
UNSTIFFENED
1 STIFFENER
3 STIFFENERS
σ x / Edge over Clamped Edge
1.0
.9
.8
.7
.6
.5
4
3
2
1
0
100
200
300
400
500
600
700
800
900
1000
1100
1200
1300
1400
1500
1600
τ xy in p.s.i.

Figure XI

Figure XII

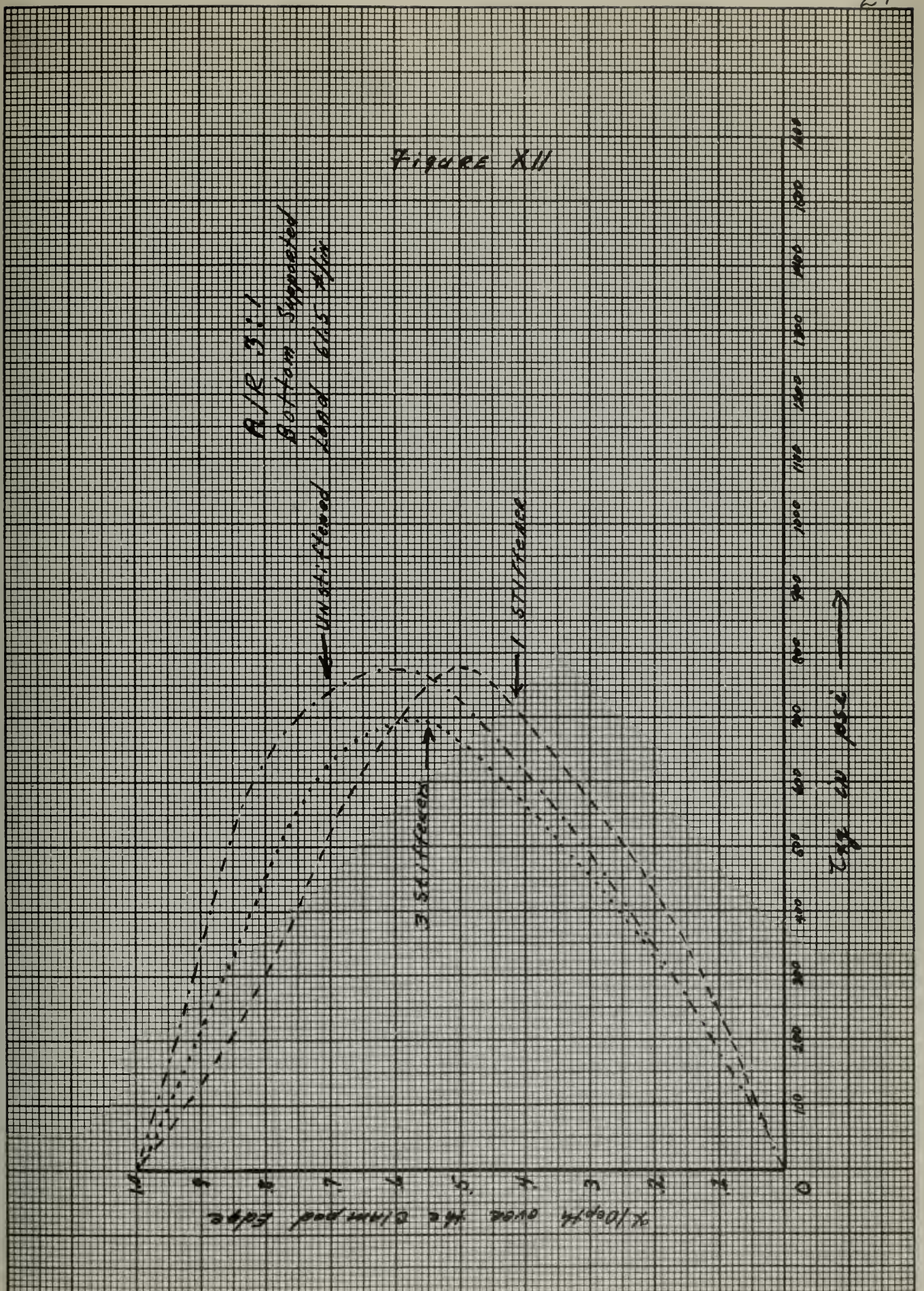
R/L 5:1
Bottom Suppressed
Top Edge
Upper Limit
Lower Limit
Left Edge
Right Edge
Maximum Stiffness
Minimum Stiffness
% Depth over the Chimney Peak Edge

Figure XIII

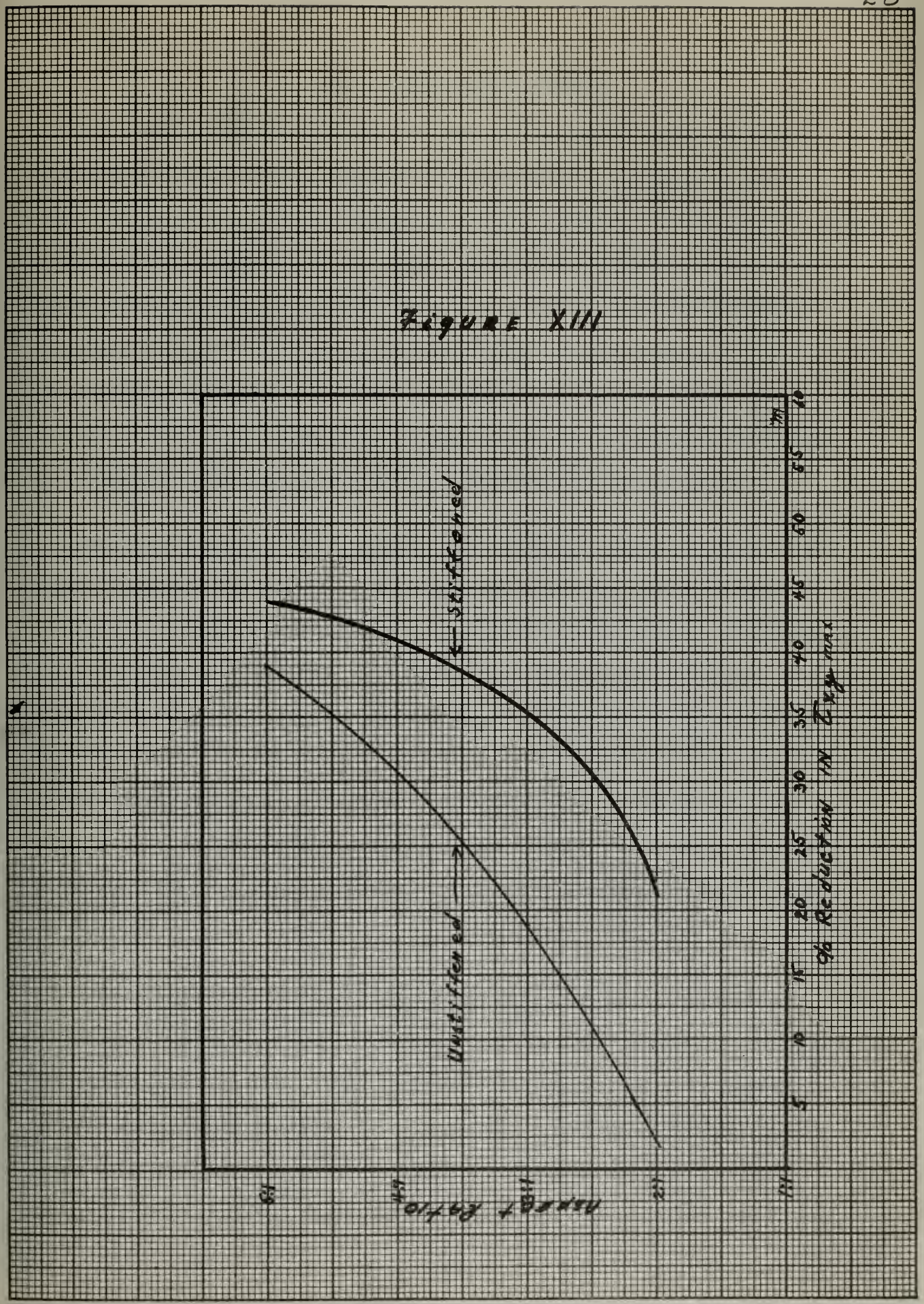
Unstrengthened
Strengthened
% Reduction in Area
Tensile Strength Ratio

IV DISCUSSION OF RESULTS

1. Isochromatic fringe patterns for each of the aspect ratios and conditions investigated were obtained by photographs of the Catalin models taken at full scale and are reproduced in the Appendix. These patterns give a qualitative indication of the stress throughout the model. It will be noted that the photographs were taken of only 1/2 of the model; however, in general the patterns were quite symetrical. In some cases, it may be seen that the isotropic point in the middle of the plate did not fall exactly on the centerline; however, limitations of the physical dimensions of the camera precluded being able to photograph the entire plate.

2. Isoclinic patterns were obtained from plexiglass models by tracing the images using the tracing table provided with the polariscope. In the case of the plates of Aspect Ratio 2:1, the isoclinic patterns throughout the model were so indistinct that it was felt inadvisable to include a complete tracing of the patterns; however, the direction of the principal stresses along the edge were determined as carefully as possible and plots of this distribution are included. While these directions must be considered the most inaccurate part of the experiments, it is still felt that the directions were obtained within the accuracy limitations stated under "7" below.

3. Having determined the variation of the direction of the principal stresses and the fringe order over the edge, the shear stress intensity was calculated over the edge. These curves were then plotted and compared. A general examination of these curves indicated that generally reliable results were obtained and the curves may be explained from elastic theory. In several of the stress distribution curves, reverse curvature was found.

An examination of the fringe patterns shows that this is to be expected in that the isochromatic lines also contain this reverse curvature. The reverse curvature in the stress distribution curve is more noticeable as the aspect ratio decreases and is apparently an indication of the departure of the plate from simple beam theory to deep beam behavior. It must be pointed out; however, that this curvature takes place in regions where the accuracy of the results are not entirely dependable as explained in "7" below.

4. Experiments to date in this field have been limited to the addition of a single stiffener at the mid-span of the model. It is felt that this stiffener would affect the results only slightly in as much as there is no vertical shear across this cross section of the plate. In order to obtain some idea of the effect of stiffeners, it is felt that systematic tests must be run using plates where the stiffeners have been added in regions of relatively high shear. As a first step in this direction, two additional stiffeners were added at the quarter points of the model with aspect ratio 3:1. The results of these tests are encouraging and indicate that the stiffeners in regions removed from the midspan of the plate do materially affect both the shear stress distribution and the value of maximum shear stress intensity. These effects are shown graphically in Figures XI and XII, and demonstrate a need for further investigation into the effects of stiffeners on plates carrying shear loading.

5. The effect of the addition of bottom support is shown in Figure XIII. These results are in general what might be expected and show decreasing effect as the aspect ratio decreases.

6. The calibration curve of the uniform loading device is shown in Figure XV. This curve is discussed as part of the results in as much as the successful design and application of this device is considered a part of this thesis. The actual load on the plate is not required in order to determine the stress distribution over the edge of the plate; however, such a calibration is needed to ascertain whether or not the load is in fact uniform and is a function of the gage pressure. In addition, this load should be known in order to furnish a check on the accuracy of the results. The intersection of the calibration curve with the ordinate of zero order is an indication of the pressure absorbed by the hoop stress in the gum rubber tube. This point may be checked by applying hydraulic pressure to an unrestrained tube. This was done and it was found that the tube ballooned at a pressure of approximately 35 to 40 psi. Above this pressure, the calibration curve showed a straight line variation of load with pressure up to a pressure of approximately 350 psi. It was assumed that this variation continued as a linear relation and the curve was extrapolated to 500 psi in order to give an indication of the accuracy of the results obtained from the experiments run at this pressure. This may or may not be a valid assumption and the calibration curve should be used with caution above a pressure of 350 psi. Pressures above 350 psi could not be obtained without running the risk of breaking the test specimen since a beam of high aspect ratio was required in order to be sure that the test model conformed to simple beam theory.

7. Accuracy: The overall accuracy of the results achieved in these experiments were determined to be 15% or less. This figure was derived by comparing the total vertical shearing force as calculated from the area under the shear stress distribution curves for the unsupported plates with the total vertical shearing force calculated from the calibration of

the uniform loading device. The uniform loading device was calibrated by two independant methods with a variation of less than 3%. It is therefore felt that the accuracy of load indications is within a maximum of 5%, the additional error due to extrapolation. Analysis of the procedures and results indicate that the majority of the error experienced is found in the determination of the direction of the principal stresses along the clamped edges, i.e., the isoclinic lines. The isoclinic lines were determined using plexiglass models rather than the catalin models used for the isochromatic fringe patterns. A comparison of the isoclinic tracings and the isochromatic photographs indicate some difference in the position of the isotropic points from which the conclusion must be drawn that there is some error in the determination of the isoclinic lines. It will be noted that a 5° error in the determination of the direction of the principal stresses in a region where the $\sin 2\theta = .5$ ($\theta = 15^{\circ}$) will give a 30% error in τ_{xy}; however, a 5° error in the determination of the direction of the principal stresses in a region where the $\sin 2\theta = 1$ ($\theta = 45^{\circ}$) gives an error in τ_{xy} of less than 1/2%. The points of maximum τ_{xy} with one exception lie in a region where the direction of the principal stresses is between 40 and 50 degrees. In this region a 5° error would give a maximum error in τ_{xy} of 4%. Therefore, it is felt that the maximum shear stress intensity as determined from the experiments is accurate with a maximum error of 9% and probably is accurate withing 5%. As points become more and more removed from the region where θ lies between 40 and 50 degrees, the accuracy of the shear stress intensity becomes less and less and little reliance can be placed on those points outside of this region.

V CONCLUSIONS

1. The method for applying a uniform load to the top edge of a plate is feasable as used in these experiments; however, experience gained during the course of this work indicates that the design of the uniform loading device could be improved with certain modifications. These modifications are discussed in Section II.

2. A general examination of the results indicate that the aspect ratios used lie in the transition range between simple beam theory and plate theory.

3. In view of the tendency of the models to exhibit unsymmetrical photoelastic patterns, accuracy could be improved by the use of smaller models so that both ends of the model could be observed and photographed at the same time.

4. For a plate of aspect ratio 5:1, the vertical shear distribution is in general parabolic, with maximum shear stress at the mid-height of the plate. With decreasing aspect ratio (3:1 to 2:1), deviation of shear stress distribution from parabolic increases, and the point of maximum shear stress intensity tends to move away from the mid-height toward the loaded edge.

5. The effect of decreasing aspect ratio for a constant uniform load is to rapidly decrease the maximum vertical shear stress intensity, and to flatten the distribution curve resulting in a less rapid variation of vertical shear stress intensity along the clamped end.

6. Results generally indicate that the addition of rigid bottom support decreases the maximum vertical shear stress intensity and the total shear over the clamped end in all aspect ratios. This decrease is most pronounced for higher aspect ratios (5:1) and less as aspect ratio decreases. This effect is intensified when the plate is stiffened.

7. The addition of a single stiffener at mid-span has little effect on the magnitude of the vertical shear stress intensity along the clamped end.

8. The addition of stiffeners at the quarter points of the plate increases the maximum vertical shear stress intensity along the clamped end when the bottom edge is unsupported, and decreases it when the bottom edge is rigidly supported.

9. The present method of clamping the ends of the plates in the straining frame is not completely satisfactory because of the inability to determine the exact point that clamping takes place, and uncertainty as to the degree of clamping achieved.

VI RECOMMENDATIONS

1. In order to achieve the long term goal, it is recommended that this work be continued with emphasis on the following:

   a. Extend the present work to include an Aspect Ratio of 1:1.

   b. Investigate the effect of additional stiffeners on the various aspect ratios for both uniform and point loading.

   c. Investigate the effect of non symetrical loading.

2. In further experiments, it is recommended that the model size be decreased to a length of six inches in order to be able to photograph the entire plate.

3. It is felt that the present system of clamping the plates in the straining frame is not completely satisfactory and that some alternate method should be devised. If the plates are shortened to a length of six inches, this will become a necessity because of the present dimensions of the straining frame.

4. It is recommended that the modifications to the uniform loading device as discussed in Section II be made in future experiments envolving the application of a uniform load.

APPENDIX

APPENDIX A

Supplementary Introduction

THEORY: The theory of elasticity has shown that in the case of plane stress, that is when the member subjected to stress is loaded and restrained uniformly over its thickness, the thickness has no effect on the magnitude or distribution of the stress. Therefore, it is possible to make a scale model of the structure, subject it to the same loads and restraints as the prototype, without scaling the thickness, and the stress distribution within the model will be exactly the same as the prototype, and the magnitude of the stress may be extrapolated to the prototype by simple scaling laws. This is important because models used for photoelastic examination must be at least a quarter of an inch thick, and this is the same order of magnitude of the thickness of a ship's bulkhead, while the other dimensions of the model are about one fiftieth of those of the prototype.

The photoelastic technique of studying the stresses within a model has become very popular since first discovered by Breuster in 1816. It has been developed over the years by such men as Neumann, Maxwell, Werthein, and Coker, and today is one of the basic tools of experimental stress analysis. Essentially, the process is quite simple. A model made of birefringent material is placed in a straining frame and a load is applied. Polarized light is then directed through the model. Snell's law states that this polarized light will be refracted by the model, and its velocity changed in proportion to the index of refraction. The birefringent property of the model causes the polarized light to be resolved into the two planes of principal stress, the velocity of transmission in each plane is dependent on the intensity of stress in the model. Therefore, the light in the two principal planes travels at different velocities, and emerges from the model out of

phase. This light then passes through an analyser, which is a polarizing device with its axis normal to the original direction of light polarization. The velocity of the light passing through the model is a continuous function, varying from point to point throughout the model. As this light passes through the analyser, the two components, one in each of the principal planes of stress and out of phase with each other, effectively either augment each other or cancel each other out, and a series of dark or colored lines are seen on the viewing screen. These lines fall into two categories:

1. Isoclinic lines. These are the locus of all points in the model where the principal planes of stress coinside with the planes of polarization of the polarizer and analyser. The lines appear as black lines when either white or monochromatic light is used. Normally, to separate these lines from the other pattern, white light is used to give maximum illumination, and a duplicate model of relatively insensitive material such as plexiglass is used. The isoclinic pattern is obtained by rotating the polarizer and analyzer simultaneously in increments of ten degrees, and the lines traced on a piece of paper on the tracing table. Thus by interpolation between the lines, the direction of the principal stress axes for any point in the model is known, and their inclination to the axes of the model is identified by the angle θ.

2. Isochromatic lines. These lines appear as colored patterns if white light is used, or as a pattern of black and white lines if monochromatic light is used. This phenomenon is called a fringe pattern, and the dark lines are called orders of interference. They are the locus of points of constant difference between principal stresses, $\sigma 1 - \sigma 2$. Since the maximum shear stress (τ_{max}) equals $\frac{\sigma 1 - \sigma 2}{2}$, these dark lines are also the locus of points of constant maximum shear stress. The isochromatic lines are

separated from the isoclinic lines by introducing quarter wave plates between the model and the polarizer and analyzer. These plates are cut to produce a relative retardation of exactly a quarter wave length of the light used. Naturally, a monochromatic light source must be used in this case, and the most common is mercury green, as produced by a mercury vapor light. This monochromatic light, therefore, passes through the polarizer and the quarter wave plate, and emerges in a condition called circular polarization. This circularly polarized light is non-directional in nature, and, therefore, will not be effected by the principal stress axes of the model. The isoclinic lines do not appear in this case, and the isochromatic lines may be observed by themselves.

It can be shown that:

$$\sigma_1 - \sigma_2 = \frac{fn}{h}$$

where: f is the fringe constant of the model material (pounds per inch-order)

n is the order of interference

h is the thickness of the model (inches)

In this experiment, it is desired to find the shear stress distribution along the clamped ends of the beams, that is the distribution of τ_{xy} at the ends, when the x axis is horizontal and the y axis is vertical. It can be also shown that:

$$\tau_{xy} = \tau_{max} \sin 2\theta$$

therefore:

$$\tau_{xy} = \frac{\sigma_1 - \sigma_2}{2} \sin 2\theta$$

or:

$$\tau_{xy} = \frac{fn}{2h} \sin 2\theta$$

"f", the fringe constant, is determined as described in the appendix under calibration,

"n," the order of interference, is determined from the isochromatic pattern, and

"θ," the angle of inclination of the principal axes to the x and y axes, is determined from the isoclinic pattern at the point desired.*

*For a more detailed discussion of the polariscope and derivation of the formulae, see reference 5.

APPENDIX B

Details of Method and Procedure

1. Preliminary

The preliminary steps involved in the procedure have been discussed in general in Section II. These consisted in aligning the polariscope and preparing the models. In addition to the normal library search which is made in preparation for a thesis, it is suggested that Course 2.126, Experimental Stress Analysis, and Course 1.561, Advanced Structural Mechanics, should be prerequisits for a thesis of this type. These two courses cover the essential elements envolved in the theory and operation of the polariscope and the Theory of Elasticity.

2. Details of Procedure

After all preliminary steps have been completed, tests on the models were carried out in the following manner. The straining frame was adjusted in height by placing wooden chocks under either end so that the model to be tested would be approximately centered in the light path of the polariscope. All bolts in the retaining channels were removed and the removable channel was taken off the frame. The uniform loading device was then placed on the frame using single bolts at either end. The model to be tested was then placed in the slot along the under side of the uniform loading device and seated securely against the rubber tube in the slot. One of the members of the thesis group then held the model in position while the other member placed steel chocks (mild steel flat bars 1" x 3/16" x width of the model) on either side of the model between the model and the channels. In order to increase the friction on the faying surfaces, strips of emery paper glued back to back were placed between each faying surface. The removable channel was placed in position and one bolt was inserted near the centerline of the model and taken up enough to hold the model in place while the other end of the model was being

rigged in a similar manner. After both sides of the model were in position, the remaining bolts were inserted and all bolts were tightened with a socket wrench as tight as possible without shearing the bolts or stripping the threads. For the first test in each aspect ratio, the model was placed in the straining frame without support along the bottom edge of the model.

With the model securely in place, the mercury arc light in the polariscope was turned on and allowed to warm up until the intensity of the light was steady. Approximately three minutes was required. While the model was being positioned, the white light was used, in as much as the expected life of the mercury arc is only some 100 hours and a replacement was not immediately available. While the mercury arc is being allowed to warm up, the hydraulic pump is attached to the uniform loading device and the size of the model image is checked on the ground glass screen. If this size needs to be adjusted it may be done by moving the ground glass screen along the camera bench tracks. When the light is steady, hydraulic pressure is slowly brought up by means of the hydraulic pump. The model is kept under observation during this procedure in order to determine if the specimen is behaving normally, to see whether or not the specimen is being loaded symetrically, and to assure that the model is not being overloaded. It may be that the model will need readjusting, in which case the bolts must be loosened and the model repositioned until the load is symmetrical.

If all was well, the load was increased to the test value pressure. In the case of the 5:1 aspect ratio, the pressure was 350 psi, the 3:1 aspect ratio was tested at both 350 psi and at 500 psi, and the 2:1 aspect ratio was tested at 500 psi. In the future, it is suggested that all aspect ratios be tested at the same load. When the test pressure was reached, the film holder was inserted in the camera and the fringe picture was taken.

The film used was Kodak Royal Ortho Cut Film in the 8 x 10 size. This film has a high sensitivity to green light, moderate grain, and normal contrast making it ideal for this type of work. Exposures were at 1/5 of a second with the aperture wide open. The small hole on the masking plate of the light source was used for all pictures. The negatives were developed immediately in the adjacent dark room to insure that the picture was obtained. The developed used was Kodax DK 60a. The film was developed using continuous agitation in a tray for the recommended four minutes. It is suggested that a better procedure would be to use the developing tanks; however, the film holders to be used in the tanks were not available in time to use. When it was assured that the picture was obtained, the negative was placed in the wash water and the testing process was continued. Later, when the negative was dry, it was printed in the 8 x 10 contact printer on Kodax Azo Contact Printing Paper, #F - 4. F-3 and F-5 were tried but it is believed best results were obtained with the F-4 paper.

When it was assured that the picture was good, the catalin model was replaced with a plexiglass model of the same dimensions. The mercury arc light was secured and the white light turned on. The ground glass screen was replaced with the isoclinic tracing table and the camera was readjusted to give the desired size of the image. The quarter wave plates were removed from the polariscope and the dark green filter was removed from the camera lens. The isoclinic pattern was then traced at 10 degree intervals, by rotating the polarizer and the analyzer together in 10 degree steps from the reference position of 90 degrees (all elements vertical) down to the horizontal. After the isoclinic pattern was traced throughout the model, the clamped edge was investigated. The edge was divided into 10 equal units with half units near the top and bottom edges. The polarizer and the

analyzer were placed at the vertical and rotated together until the darkest portion of the isoclinic was over the marked points on the edge. This value of the angle was recorded. After the angular value for all points had been determined, the curve of angle versus station along the boundary was plotted. These curves are included in the Appendix. If there were any points which did not fall on a smooth curve, these points were rechecked until a smooth curve was obtained. This completed the test for the unsupported and unstiffened condition.

The plexiglass plate was then removed and the unstiffened catalin plate was placed in the straining frame with a rigid support under the bottom edge. An aluminum bar, 1/2 inch wide by 2 1/2 inches deep was placed under the edge of the plate. A thin piece of cardboard was placed between the bar and the bottom edge. The uniform loading device was placed over the top edge of the plate and firmly seated with the rubber tube against the top edge of the plate. The holes of the uniform loading device were bored on 3/4 inch centers while the holes in the restraining channels on the frame were spaced on 7/8 inch centers. By making use of this vernier principal one set of holes on the loading device was always approximately in line with a set of holes on the channels. A slight adjustment could be made by placing an additional cardboard shim under the bar providing bottom support. The same procedure was then followed to obtain the fringe pattern photograph and the angular variation of the direction of the isoclinics lines over the clamped edge.

After the model was investigated without stiffeners for the two conditions of bottom support, a stiffener was glued to the centerline of the plate. This stiffener was made up of two strips of catalin, 1/4 inch by 3/8 inch by the width of the plate minus about 1/4 inch at the top. The 1/4 inch allowance at the top was made in order to allow the top edge of the model to slip into the slot in the uniform loading device. One of these strips was

glued on each side of the plate to prevent bending from being introduced. The glue used to make the joint was Penacolite Adhesive G-1124 manufactured by the Koppers Company, Inc., Pittsburg, Pennsylvania. This glue has the action of penetrating into the catalin and effectively forming a welded joint. The glue is a two part glue which must be mixed just before it is applied. One part is a resin filler and the other is an activator and a solvent. The glue is mixed in the ratio of one part solvent to three parts resin by weight. After the glue has been thoroughly mixed both sides of the faying surface to be joined are evenly spread with a thin coating of the glue and allowed to dry for a period of ten minutes. The two surfaces are then brought into contact and pressed together using C clamps. The excess glue which is squeezed out of the joint may be cleaned off using a piece of cotton soaked in acetone. After the joints were formed and cleaned, the model was allowed to dry for a period of 24 hours. The tests as described above were then repeated for the model with stiffener added. In the case of the 3:1 aspect ratio model, additional stiffeners were added at the quarter points after the tests with the single stiffener were completed.

3. Sample Calculation

After the angular distribution of the direction of the isoclinics lines over the clamped edge had been determined and a similar distribution of the order of interference (fringe orders) over the clamped edge had been obtained from the fringe pattern photograph, the vertical shear stress intensity was calculated at each of the 10 stations on the edge. The vertical shear stress intensity was calculated using the formula;*

$$\tau_{xy} = \frac{fn}{2h} \sin 2\theta = 173.3\, n \sin 2\theta$$

*The derivation of this formula may be found in reference 5.

The factors 1/2, f, and h may be combined into a constant. Arranging the values of order number and angle in tables as in Table III, the value of shear stress intensity, τ_{xy}, is then computed by multiplying the values of the constant, the order number, and the sin 2 θ.

The value of shear stress over the edge is then plotted for each of the calculated points. The total vertical shear force at the edge is then computed by taking the area under the τ_{xy} curve over the edge. This was done using Simpson's Rule which may be written;

$$A = \frac{s}{3}(y_o + 4y_1 + 2y_2 + 4y_3 + \cdots 2y_{n-2} + 4y_{n-1} + y_n)$$

To obtain an idea of the overall accuracy of the experiment, this calculated value of total vertical shear force may be compared with 1/2 the total load on the plate as determined from the calibration curve of the uniform loading device in the case of the models tested without bottom support. Where the models were tested with bottom support, this comparison means little in that a good bit of the total load is carried by the bottom support and not transmitted to the straining frame by shear in the model.

APPENDIX C

Calibration

1. Determination of Fringe Constant: The fringe constant of the material used (Catalin 61-893) is substantially constant; however, there is about a 5% variation from batch to batch, and it is customary to calibrate the material by determining the fringe constant for each group of models.

A standard tinsile test specimen is manufactured from a sample of the material. This specimen is placed in a straining frame and a load applied. The polariscope is set up for a light field so that it will be easier to observe the orders of interference. Since the specimen is in pure tension, the orders appear over the entire specimen, and it is very easy to observe and count them. The load applied is measured with a standard Baldwin load cell, and the load is recorded for each order, both loading and unloading. The process was repeated three times and the values averaged. The result was f = 86.3 pounds per inch-order. The handbook value is 86, which means that this batch of Catalin did not vary more than 1% from the average.

The value of the fringe constant was obtained in the following way. It has been previously stated that the fringe constant may be defined thus:

$$f = \frac{(\sigma_1 - \sigma_2)\, h}{n}$$

In the case of pure tension, σ_2 is equal to zero because the only stress is axial. The axial stress, σ_1 equals the load applied (P) divided by the area of the specimen (bxh, where b is the width and h the thickness of the specimen).

Therefore:

$$f = \frac{P \times h}{b \times h \times n} = \frac{P}{n} \times \frac{1}{b}$$

The quantity P/n is the load per order, and may be interpreted as the slope of a plot of P vs n. Therefore, the average load for each order is plotted

against order number, and the slope of the resulting straight line is substituted into the above equation and solved for "f". This then is the value of "f" that is used for all calculations in this thesis.

TABLE I

Determination of Fringe Constant

Potentiometer Reading (u ins/in, 10 u ins/in. = 1 lb.)

	RUN #1		RUN #2		RUN #3		
ORDER	UP	DOWN	UP	DOWN	UP	DOWN	AVERAGE
0	----	10-1110	10-1110	10-1110	10-1110	10-1110	11110
1	----	10-1250	10-1220	10-1220	10-1220	10-1150	11212
2	----	10-1630	10-1630	10-1600	10-1610	10-1560	11606
3	12-0100	12-0050	12-0070	12-0040	12-0050	10-1990	12050
4	12-0510	12-0510	12-0500	12-0510	12-0470	12-0440	12490
5	12-0910	12-0920	12-0950	12-0910	12-0980	12-0840	12903
6	12-1360	12-1350	12-1350	12-1340	12-1320	12-1290	13335
7	12-1790	12-1770	12-1780	12-1790	12-1740	12-1730	13767
8	14-0230	14-0200	14-0190	14-0170	14-0160	14-0160	14185
9	14-0660	14-0630	14-0640	14-0650	14-0590	14-0610	14630
10	14-1040		14-1030		14-1010		15025

Tensile Specimen: b = 0.493"

h = 0.263"

Baldwin SR-4 Strain Indicator Type L, Serial H-59248.

Baldwin SR-4 Load Cell Type u, Serial 500.

FIGURE XIV

DETERMINATION OF FRINGE CONSTANT

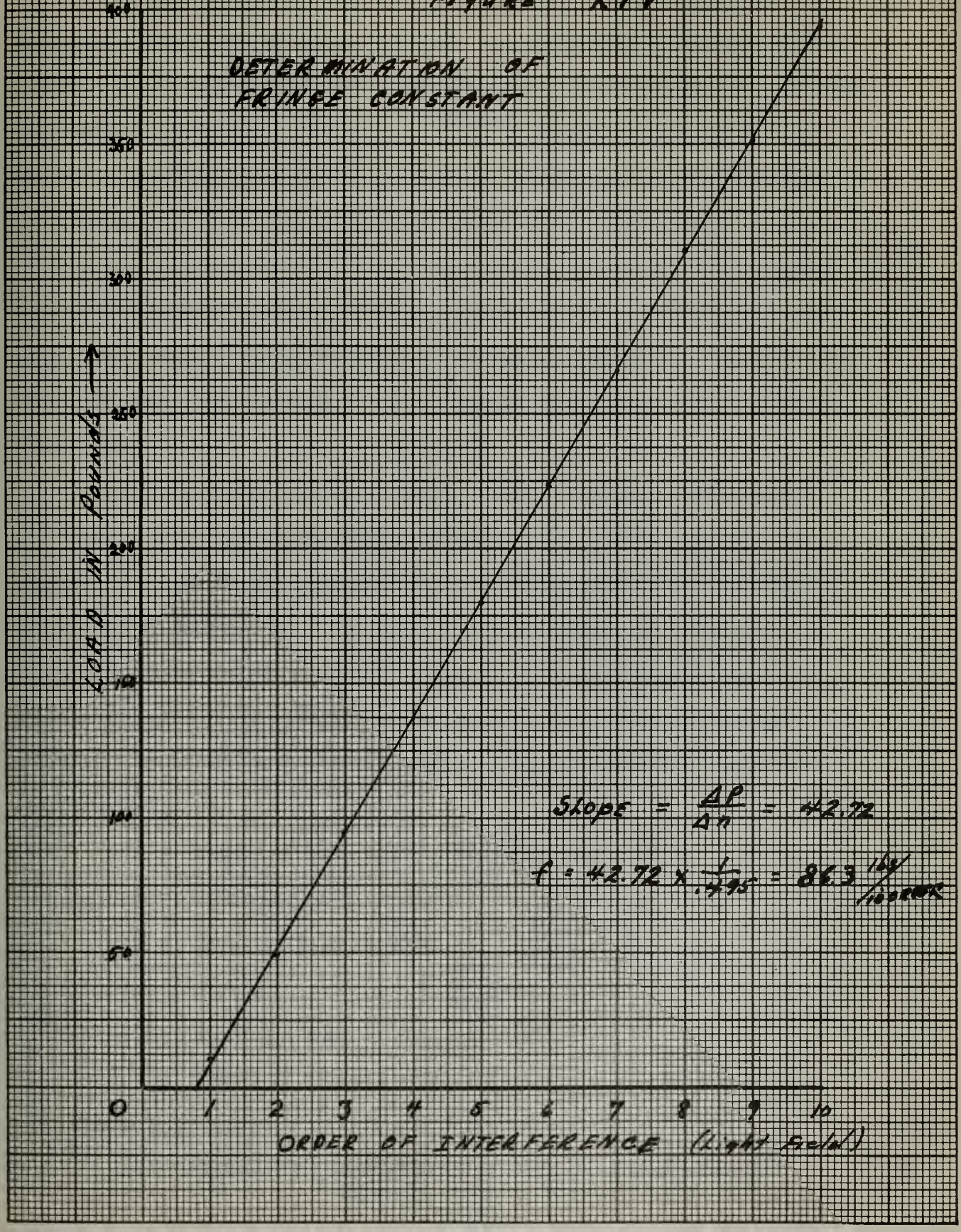

$$\text{Slope} = \frac{\Delta P}{\Delta n} = 42.72$$

$$f = 42.72 \times \frac{1}{.495} = 86.3 \ \frac{\text{lbs}}{\text{inch-order}}$$

2. Calibration of the Uniform Loading Device: The uniform loading device was calibrated by three methods. The first method used was that of a bar in pure compression. The compression bar was 12 inches long, 2 inches deep and 1/4 inch thick, and set up in the straining frame so that the top was uniformly loaded and the bottom was rigidly supported. Maximum load failed to produce one order of interference, so this was not considered sufficient for calibration, in spite of the fact that fractional orders could have been obtained by the Tardy Method. (see ref. 5) This method only served to indicate that there was a uniform load applied, since the compression bar appeared to be of uniform shade as viewed through the polariscope.

The second method utilized a simple beam in bending. The samebar (12" x 2" x 1/4") was simply supported on 11 inch centers, and the load applied. As each fringe passed a mark 3/4 inch down from the mid-height, the pressure was recorded, Ten orders were observed, and although this did not complete the range of pressures, the test was stopped for fear of exceeding the yield strength of the model. The stress at this point was calculated by photoelastic theory, and the load per inch was calculated by simple beam theory.

Let: l = length of beam between supports (in inches)

h = Thickness of beam (0.25")

d = Depth of beam (1.906")

σ_x = Stress at point y = 0.75"

M = Bending moment at mid-span = $wl^2/8$

I = Moment of inertia of cross section = $hd^3/12$

From simple beam theory:

$$\sigma_x = \frac{0.75M}{I} = \frac{1.125\ wl^2}{hd^3}$$

From photoelastic theory:

$$f = \frac{(\sigma_x - \sigma_y)\, h}{n} \qquad \sigma_y = o$$

$$\sigma_x = \frac{nf}{h} = 86.3 \ \frac{n}{h}$$

Therefore:

$$\frac{1.125\ wl^2}{hd^3} = \frac{86.3\ n}{h}$$

$$w = 4.40\ n \ \text{lbs/inch}$$

The results were plotted, gage pressure versus uniform load, and a straight line calibration curve was achieved, (see Figure XV).

The third method used was very much the same as the second except that one of the supports of the beam was replaced with a Baldwin SR-4 load cell. Knowing one of the reactions (R_1), the uniform load was calculated by statics, and this too was plotted on the calibration curve, with very good correlation. Since in this test, the supports were closer together, the pressure could be raised to 365 psi, which extended the calibration curve to a higher range than was obtained from the second method, which decreased the probable error from extrapolation, since the experiments were run at 350 psi and 500 psi.

Data for the second and third method is shown in Table II, and the calibration curve is hown in Figure XV.

TABLE II

Calibration of Uniform Loading Device

Second Method

$$w = 4.40\ n$$

Order (n)	Pressure (psi)	w (lbs/inch)
0	0	0
1	65	4.40
2	90	8.80
3	110	13.20
4	135	17.60
5	160	22.00
6	180	26.40
7	205	30.80
8	225	30.80
9	245	39.60
10	270	44.00

Third Method

Order	Pressure	R_1 (lbs)	w (lbs/inch)
0	0	0	0
1	160	120	20.8
2	265	239	41.3
3	365	356	61.5

$$w = \frac{R_1 \times 6.76}{12 \times 3.26} = 0.173\ R_1$$

Baldwin SR-4 Strain Indicator Type L, Serial H-59241.

Baldwin SR-4 Load Cell Type u, Serial 500.

Figure XV

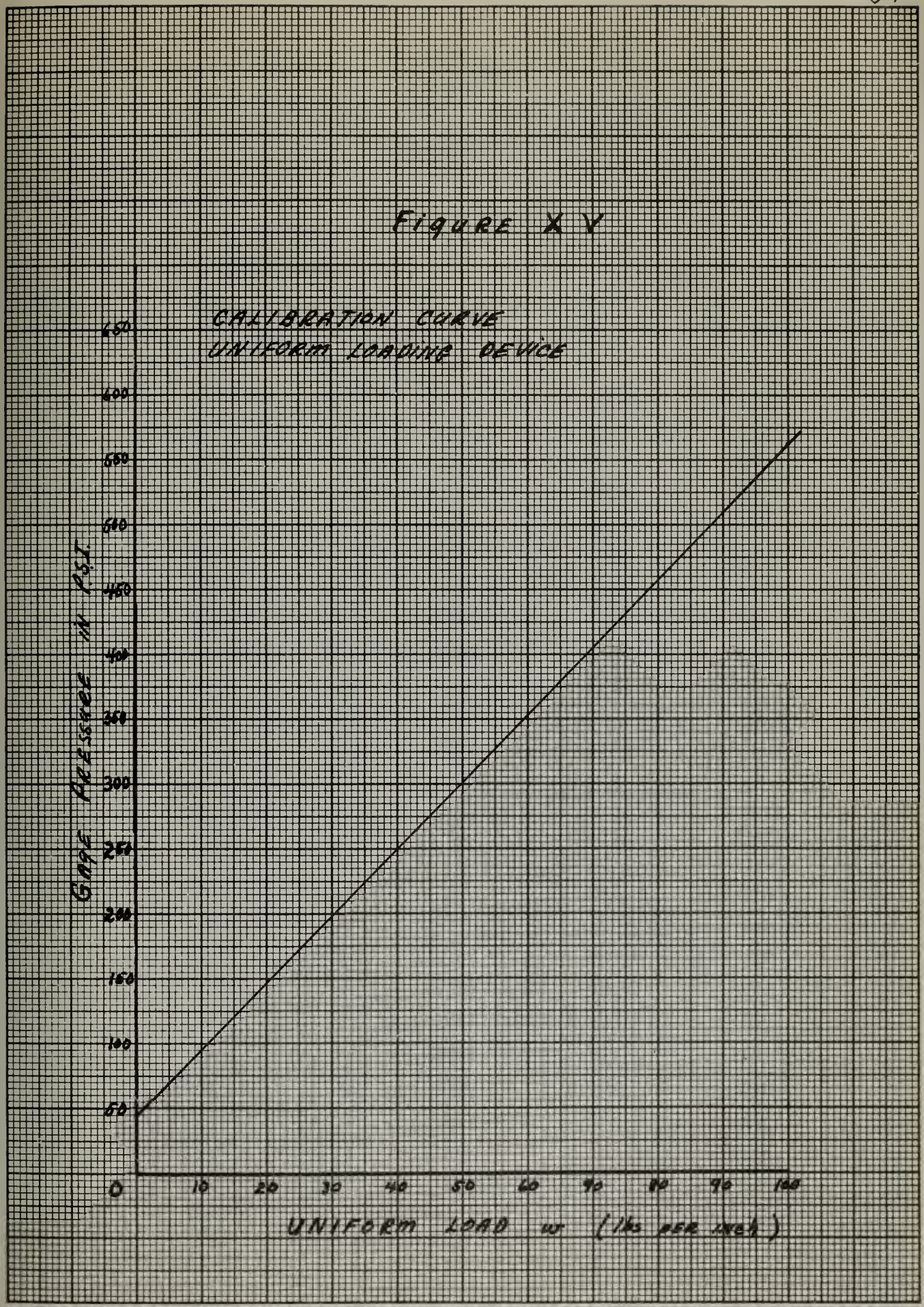
CALIBRATION CURVE
UNIFORM LOADING DEVICE
Gage Pressure in P.S.I.
650
600
550
500
450
400
350
300
250
200
150
100
50
0
10
20
30
40
50
60
70
80
90
100
UNIFORM LOAD w (lbs per inch)

APPENDIX D

Original Data and Calculations

TABLE III

Aspect Ratio 5:1

Plate Unstiffened

Bottom Unsupported Load 350 psi

Station	Order	θ	2θ	Sin 2θ	τ_{xy}
0	5.4	0	0	0	0
1/2	5.5	5	10	.174	166
1	5.9	10	20	.342	350
2	6.2	20	40	.643	690
3	6.5	30	60	.866	975
4	6.5	38	76	.970	1090
5	6.0	45	90	1.000	1040
6	5.1	51	102	.978	865
7	4.1	60	120	.866	615
8	3.1	70	140	.643	345
9	2.1	80	160	.342	125
9 1/2	2.0	85	170	.174	60.2
10	1.5	90	180	0	0

Bottom Supported Load 350 psi

Station	Order	θ	2θ	Sin 2θ	τ_{xy}
0	2.4	0	0	0	0
1/2	2.1	18	36	.588	214
1	2.1	28	56	.829	301
2	2.8	37	74	.960	465
3	3.4	41	82	.989	582
4	3.8	45	90	1.000	659
5	4.1	50	100	.985	700
6	4.2	54	108	.950	691
7	4.0	60	120	.866	601
8	3.2	67	134	.720	399
9	2.4	77	154	.439	182
9 1/2	2.0	83	166	.242	83.9
10	1.6	90	180	0	0

FIGURE XVI

ASPECT RATIO 5:1 UNSTIFFENED, UNREINFORCED

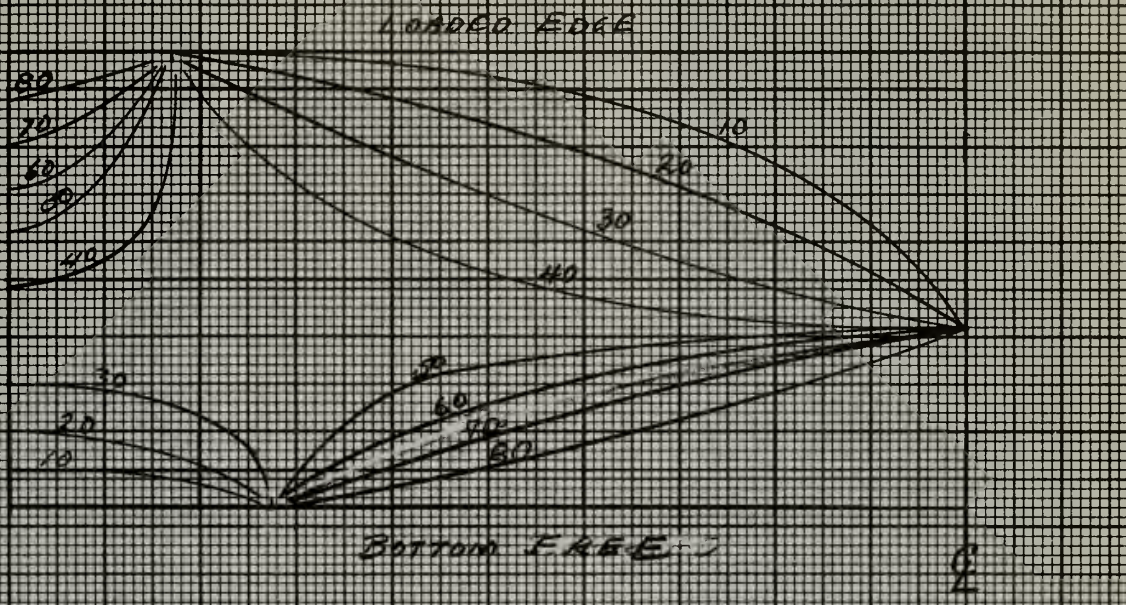

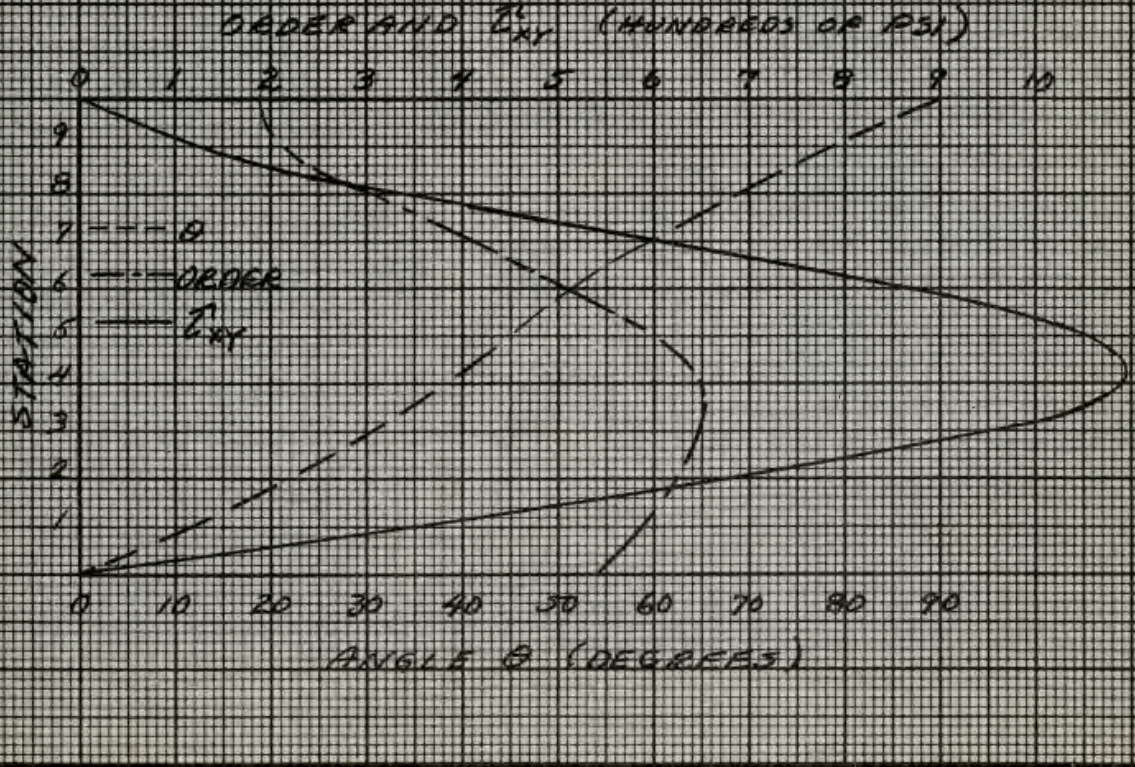

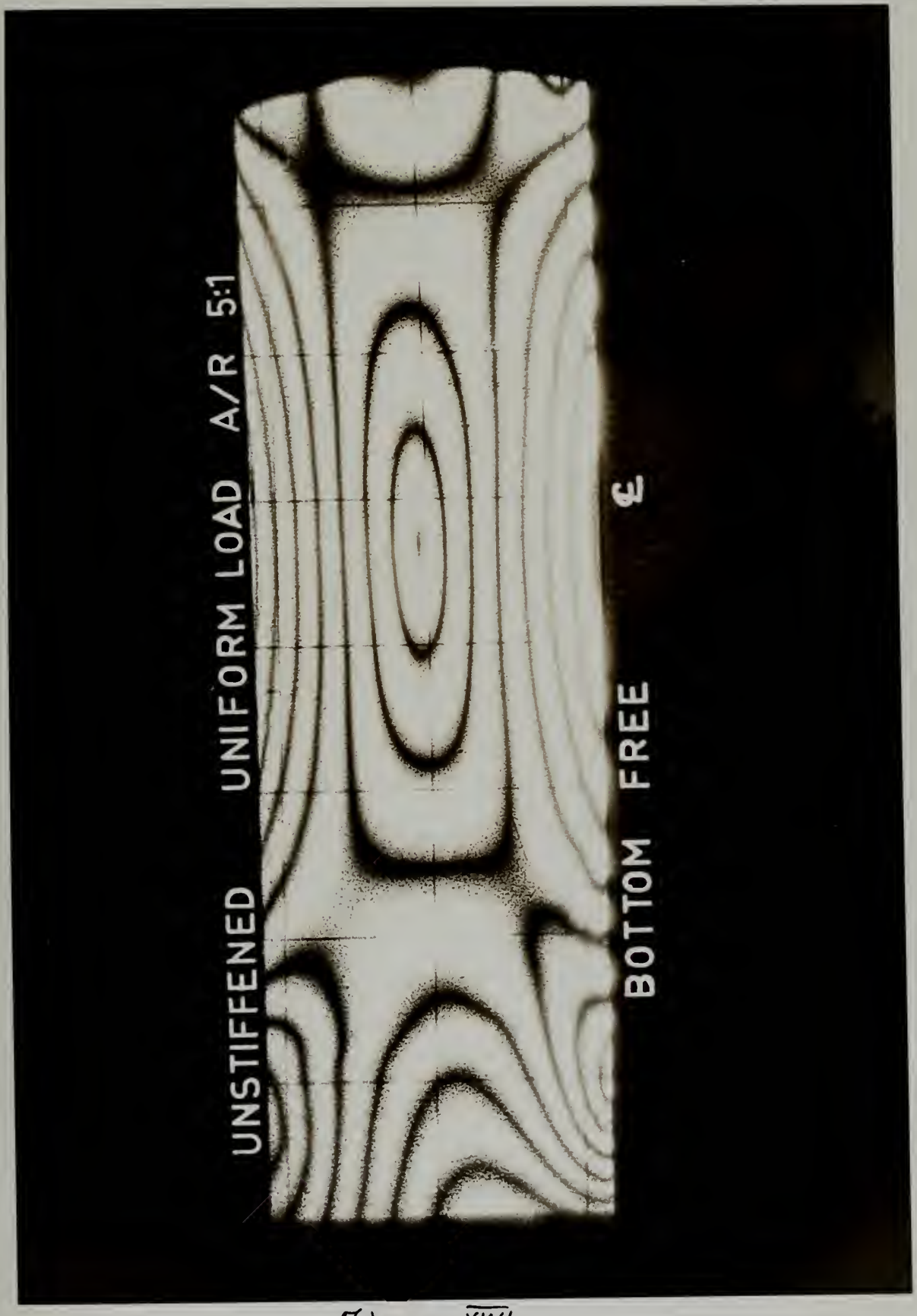

Figure XVII

FIGURE XVIII

ASPECT RATIO 5:1 UNSTIFFENED & SUPPORTED

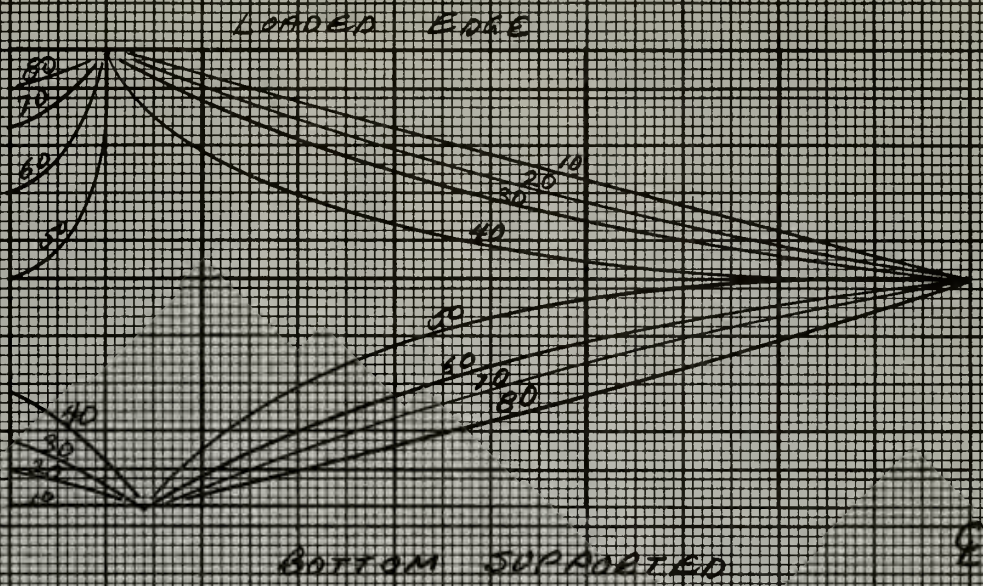

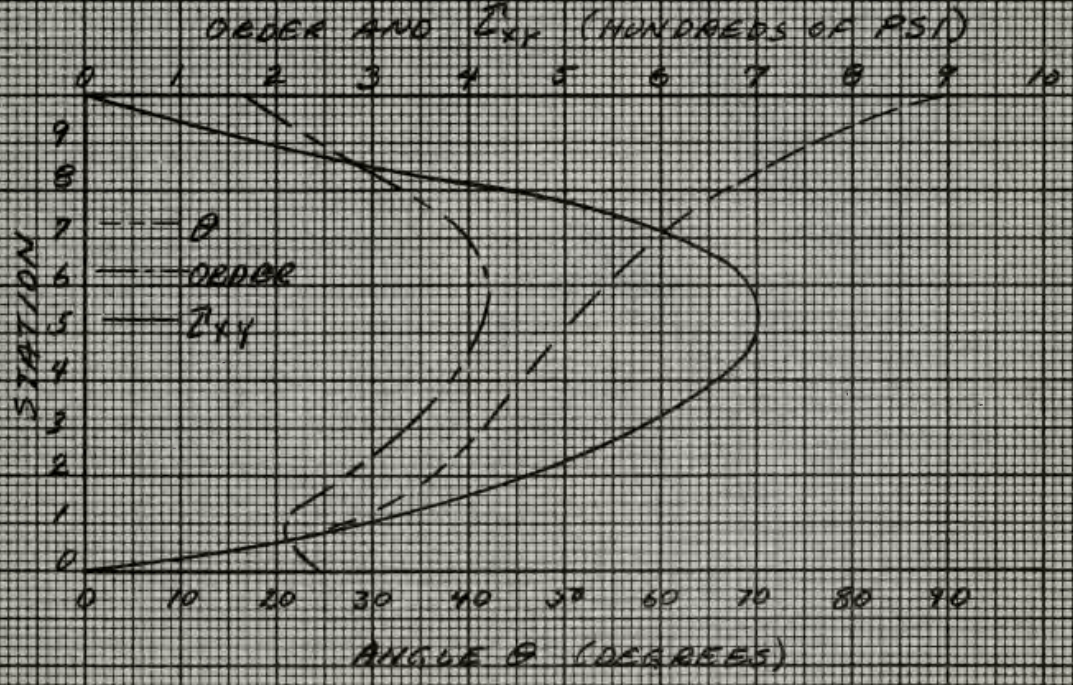

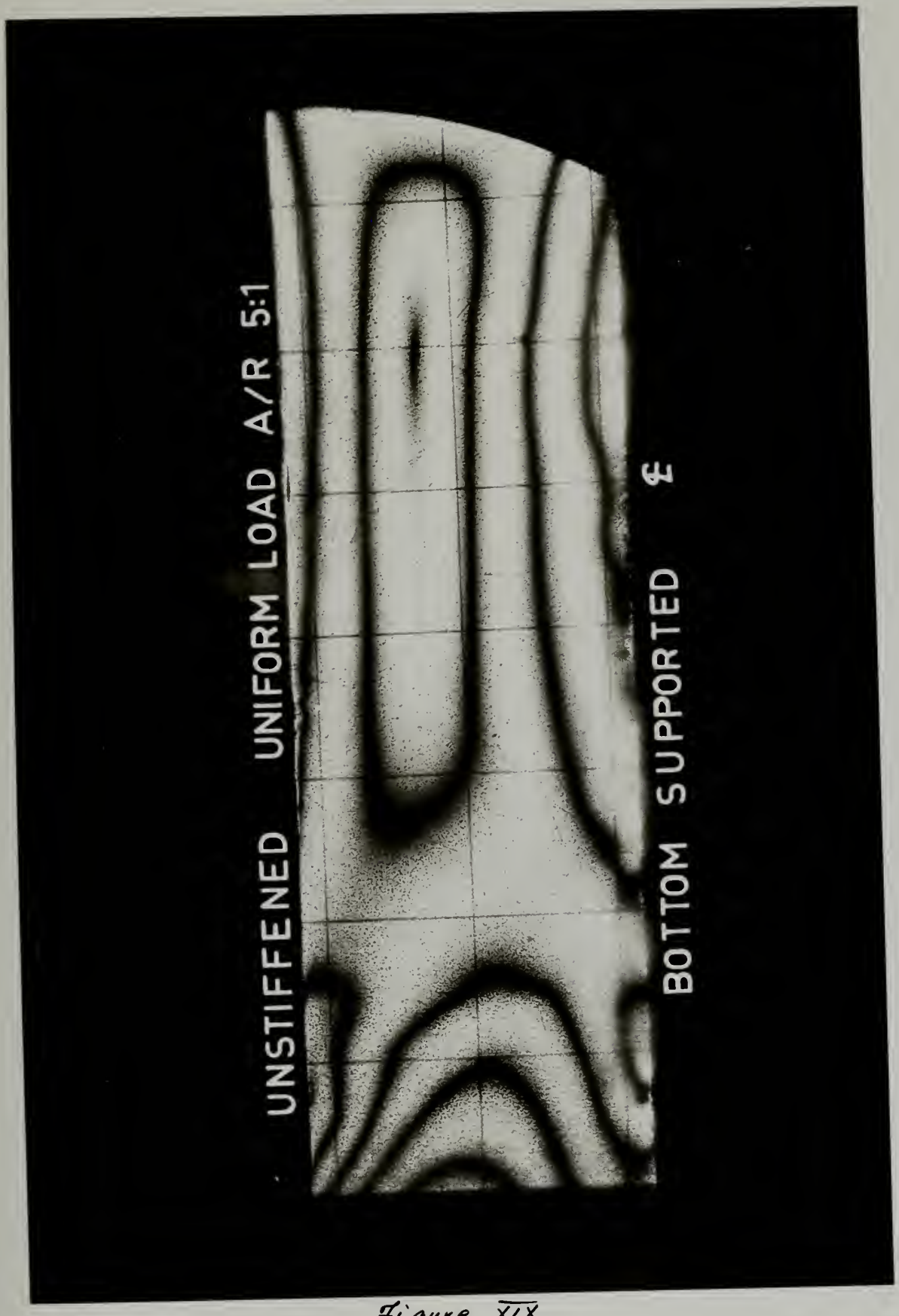

Figure XIX

TABLE IV

Aspect Ratio 5:1

Plate Stiffened

Bottom Unsupported Load 350 psi

Station	Order	θ	2θ	Sin 2θ	τ_{xy}
0	2.8	0	0	0	0
1/2	2.9	11	22	.375	189
1	3.1	21	42	.669	360
2	4.0	32	64	.900	625
3	5.1	40	80	.985	870
4	6.4	44	88	.999	1110
5	7.2	47	94	.996	1240
6	7.2	50	100	.985	1230
7	6.8	53	106	.961	1130
8	5.5	58	116	.899	856
9	4.1	70	140	.644	451
9 1/2	4.0	79	158	.375	260
10	3.6	90	180	0	0

Bottom Supported Load 350 psi

Station	Order	θ	2θ	Sin 2θ	τ_{xy}
0	2.4	0	0	0	0
1/2	2.5	13	26	.438	190
1	2.7	21	42	.669	312
2	3.0	31	62	.884	438
3	3.5	39	78	.980	594
4	3.9	44	88	.999	674
5	4.1	48	96	.994	707
6	4.1	52	104	.970	688
7	3.9	57	114	.914	617
8	2.9	65	130	.765	384
9	1.7	77	154	.438	129
9 1/2	1.0	84	168	.208	36.0
10	0.8	90	180	0	0

FIGURE XI

ASPECT RATIO 5:1 STIFFENER & UNSUPPORTED

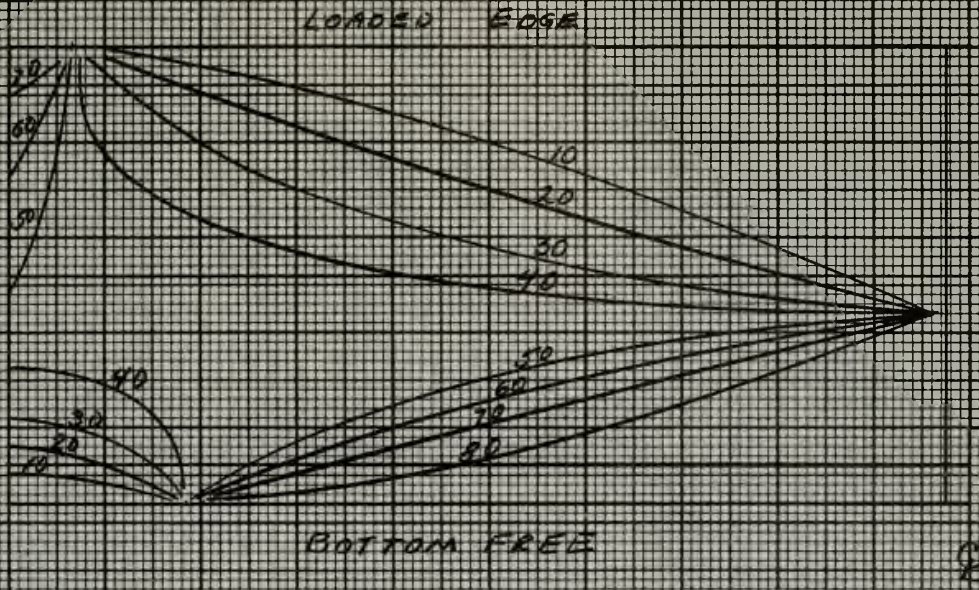

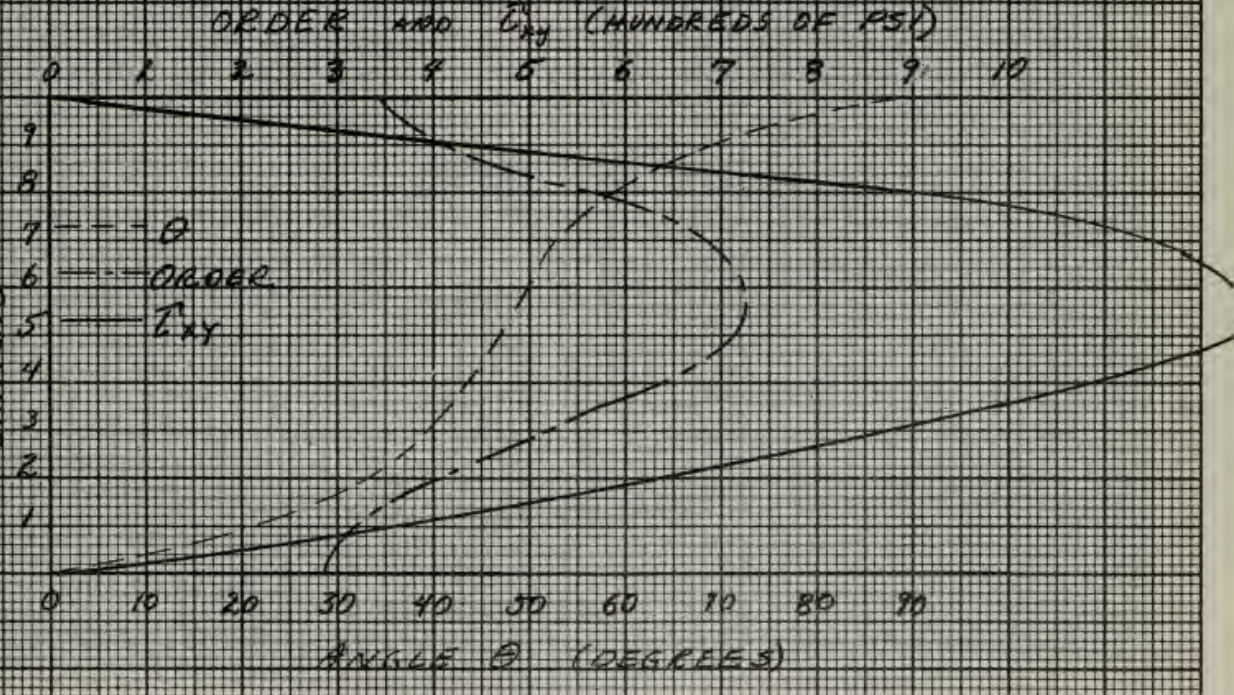
ORDER AND $\bar{\sigma}_{xy}$ (HUNDREDS OF PSI)
0 1 2 3 4 5 6 7 8 9 10
STATIONS
9 8 7 6 5 4 3 2 1
θ
ORDER
$\bar{\tau}_{xy}$
0 10 20 30 40 50 60 70 80 90
ANGLE θ (DEGREES)

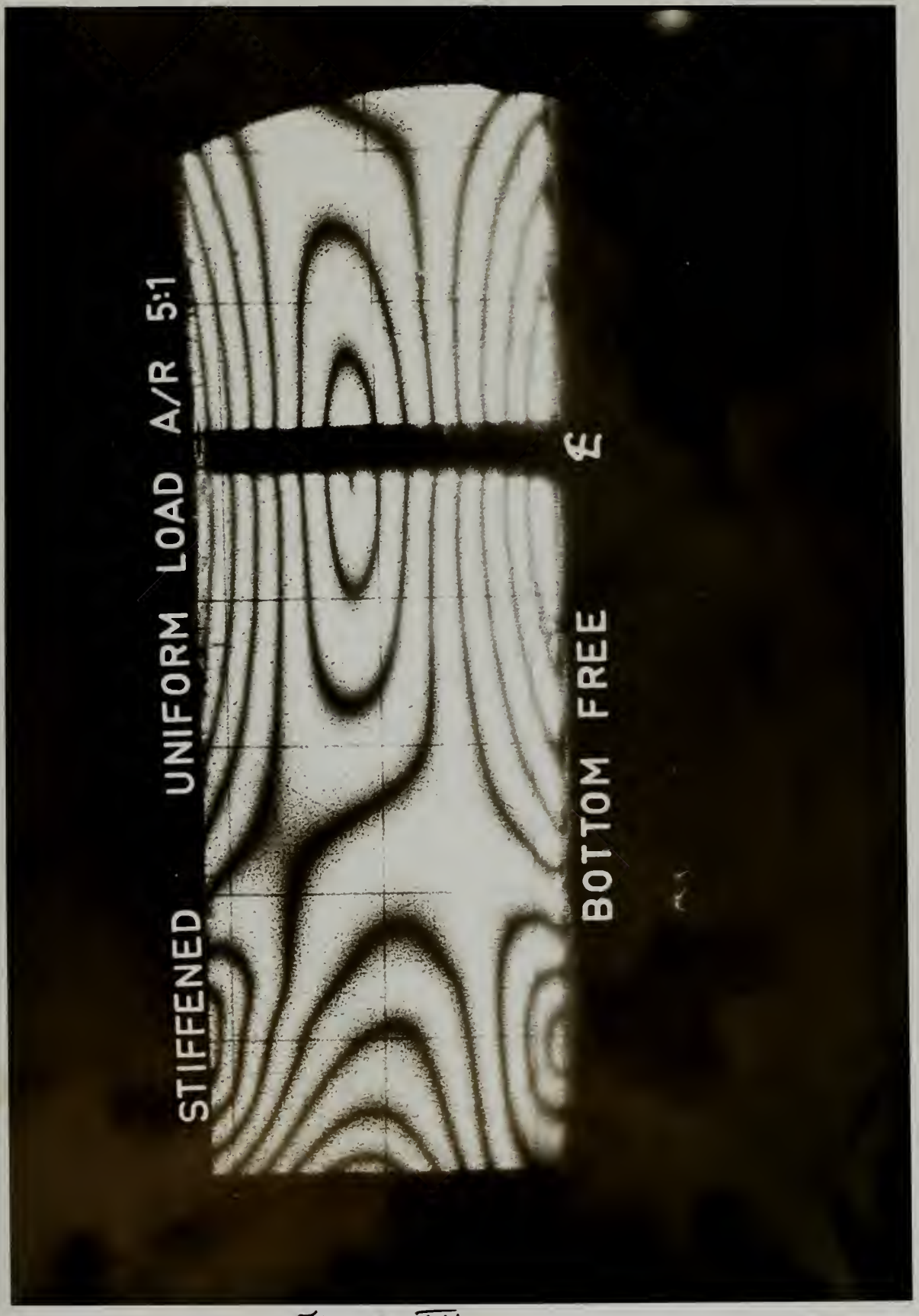

Figure XXI

FIGURE XXII

ASPECT RATIO 5:1 STIFFENED & SUPPORTED

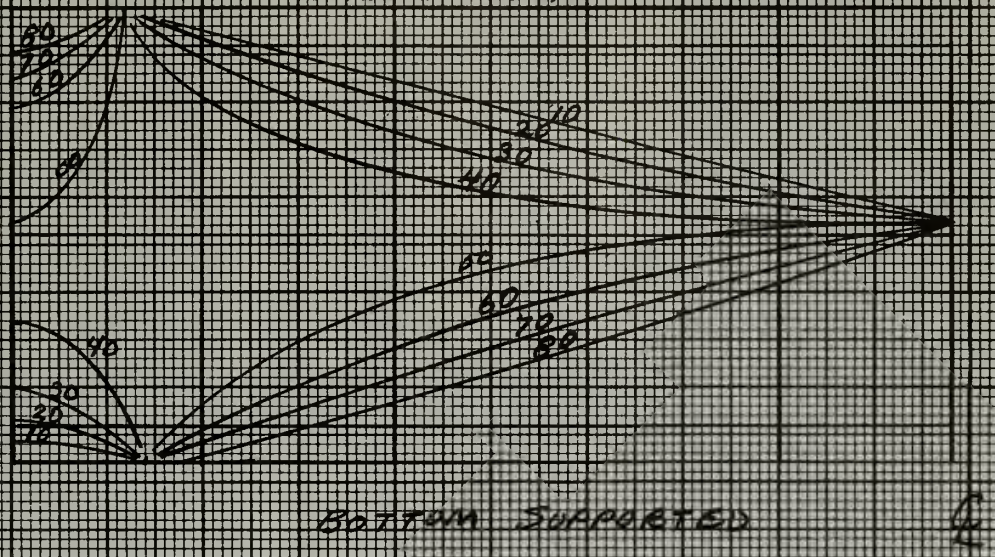

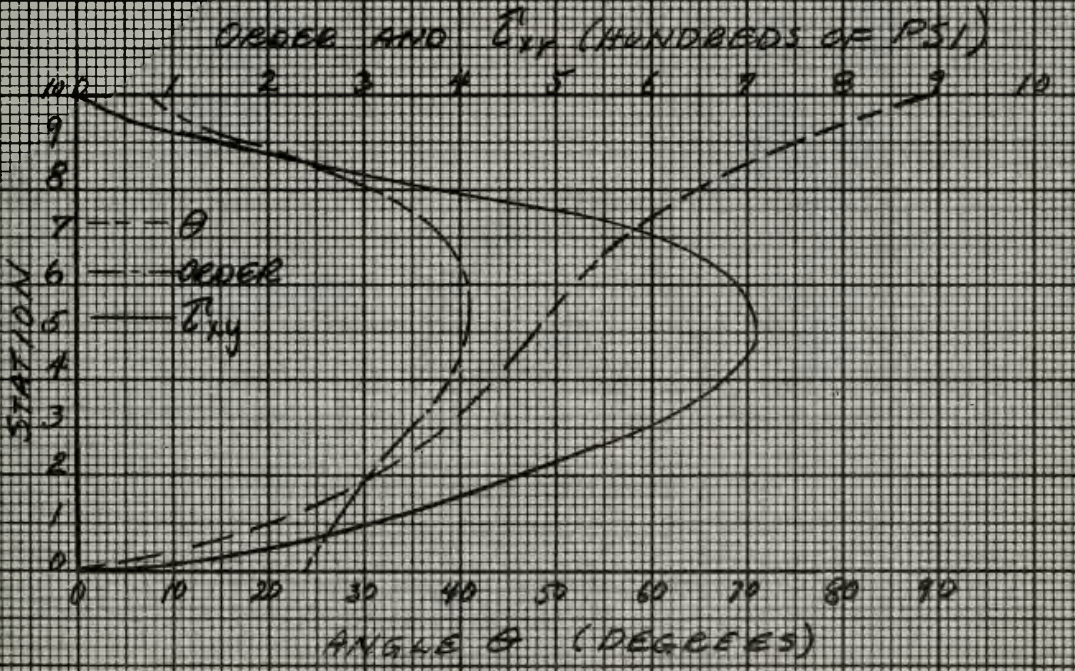

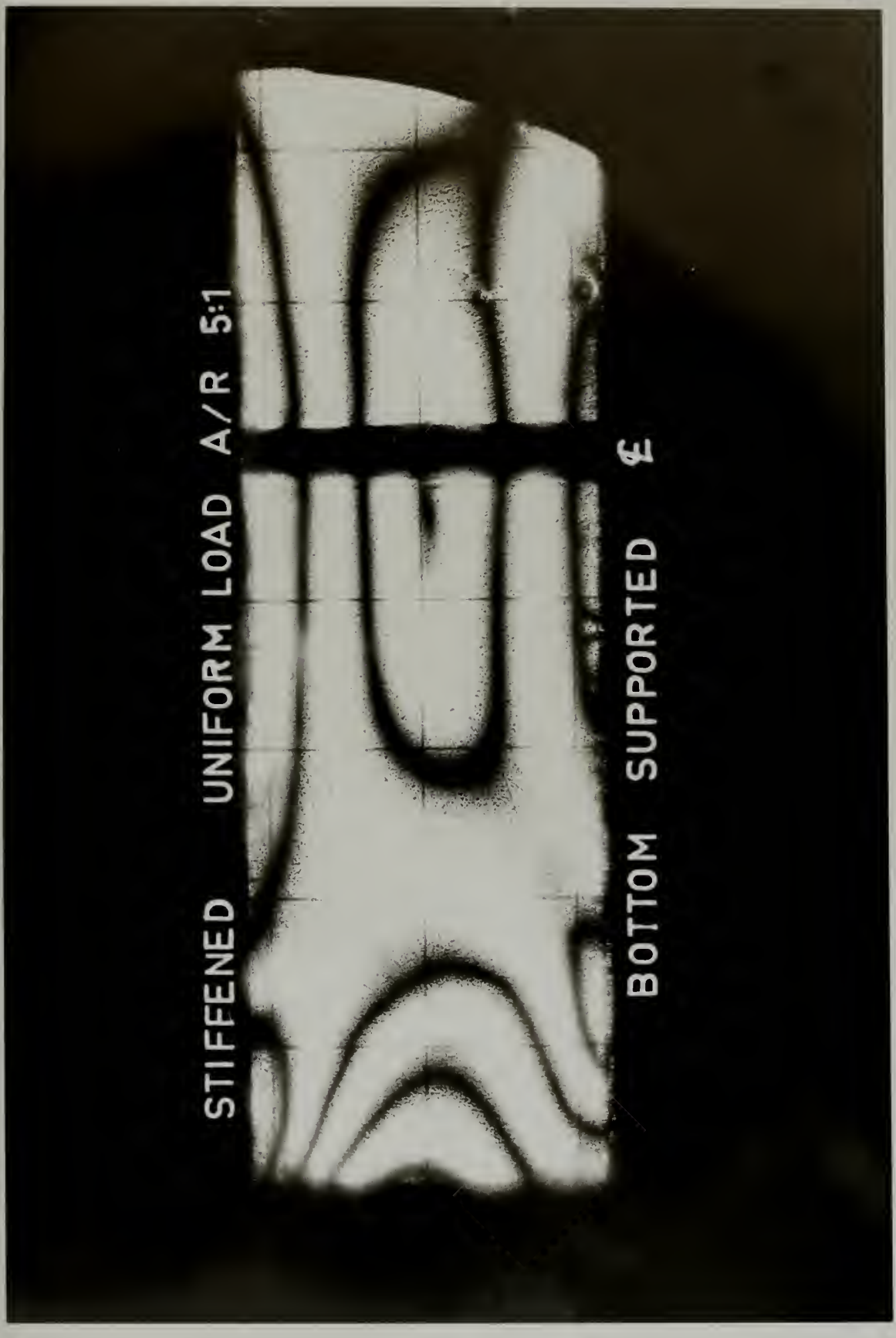

FIGURE XXIII

TABLE V

Aspect Ratio 3:1

Plate Unstiffened

Bottom Unsupported — Load 500 psi

Station	Order	θ	2θ	Sin 2θ	τ_{xy}
0	5.5	0	0	0	0
1/2	5.1	20	40	0.643	568
1	4.8	26	52	0.788	683
2	4.5	34	68	0.927	723
3	4.8	40	80	0.985	818
4	5.1	45	90	1.000	884
5	5.6	49	98	0.989	960
6	5.3	53	106	0.962	884
7	5.0	57	114	0.914	792
8	4.3	62	124	0.830	617
9	3.2	69	138	0.669	371
9 1/2	2.5	75	150	0.500	216
10	2.0	90	180	0	0

Bottom Supported — Load 500 psi

Station	Order	θ	2θ	Sin 2θ	τ_{xy}
0	1.5	0	0	0	0
1/2	1.2	13	26	0.438	91.2
1	1.4	22	44	0.695	168.0
2	2.1	32	64	0.900	327
3	2.9	36	72	0.952	478
4	3.6	40	80	0.985	614
5	4.0	43	86	0.997	691
6	4.5	46	92	0.998	779
7	4.3	51	102	0.979	729
8	4.0	57	114	0.915	634
9	2.9	68	136	0.695	349
9 1/2	2.0	75	150	0.500	173
10	1.0	90	180	0	0

FIGURE XXIV

ASPECT RATIO 3:1 UNSTIFFENED & UNSUPPORTED

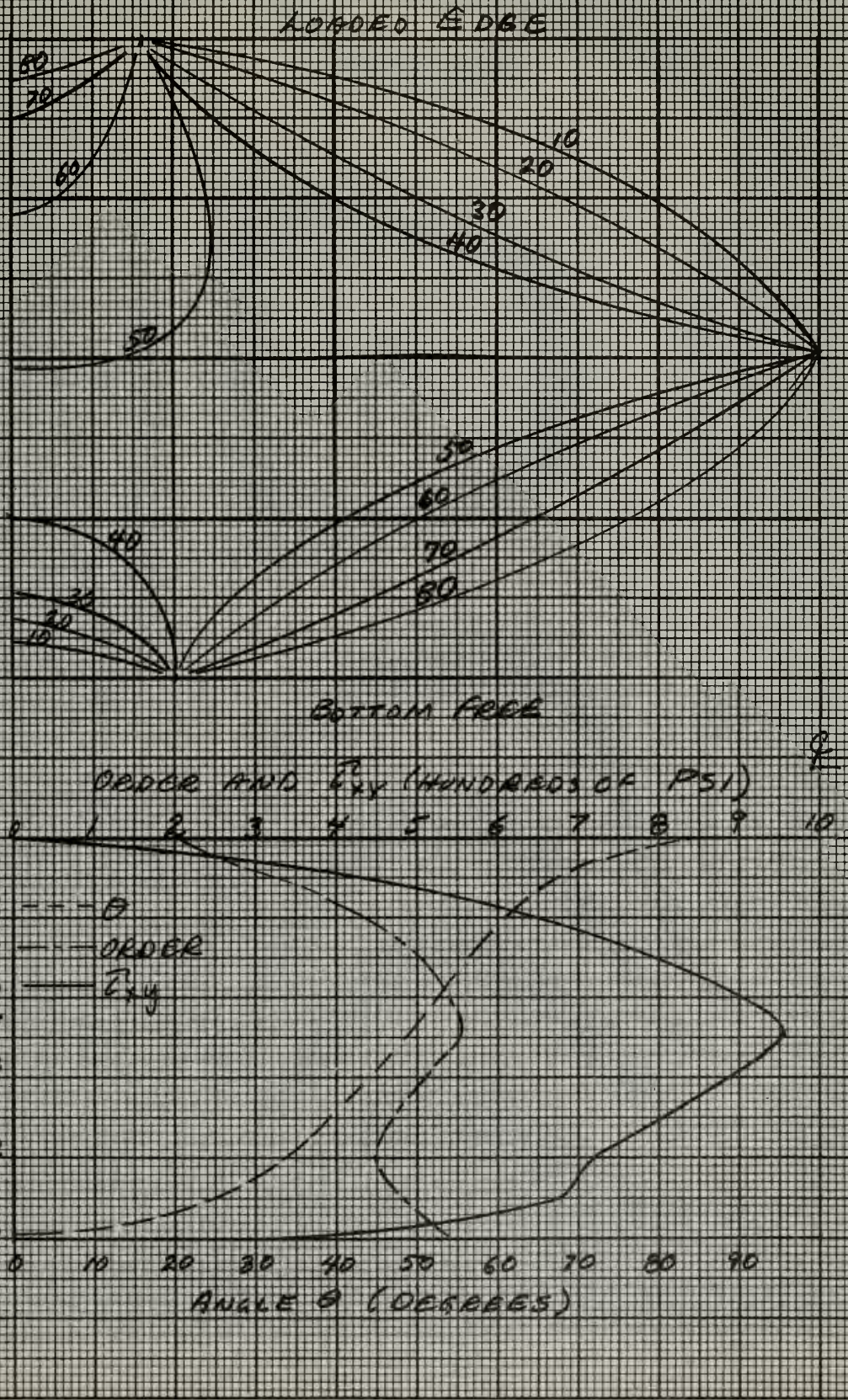

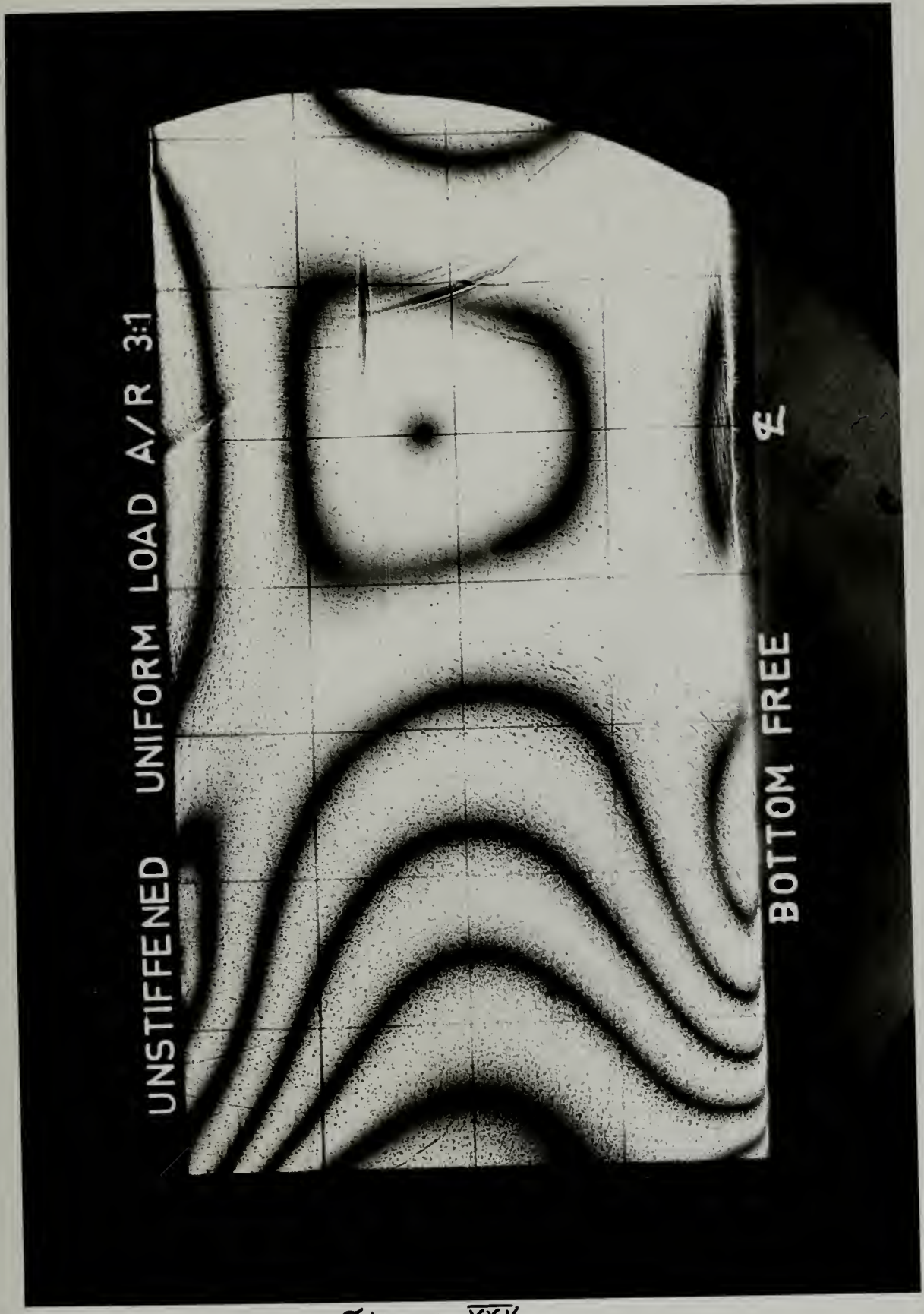

Figure XXV

FIGURE XXVI

ASPECT RATIO 3:1 UNSTIFFENED & SUPPORTED

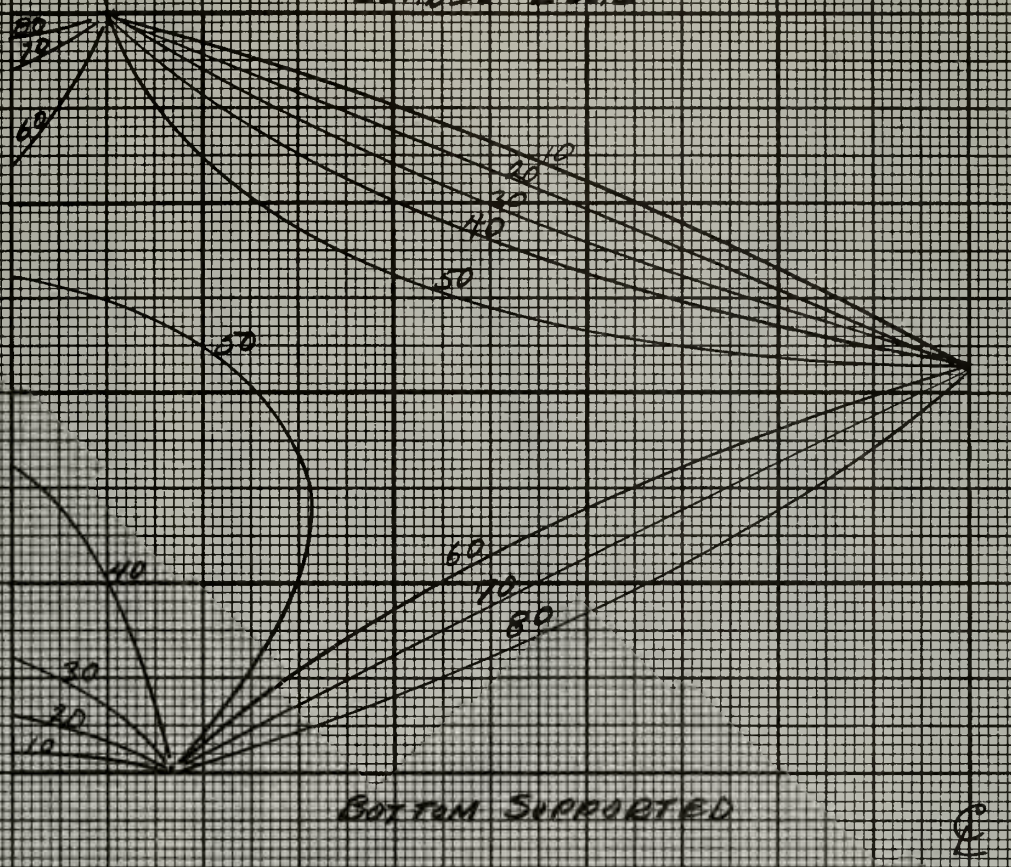

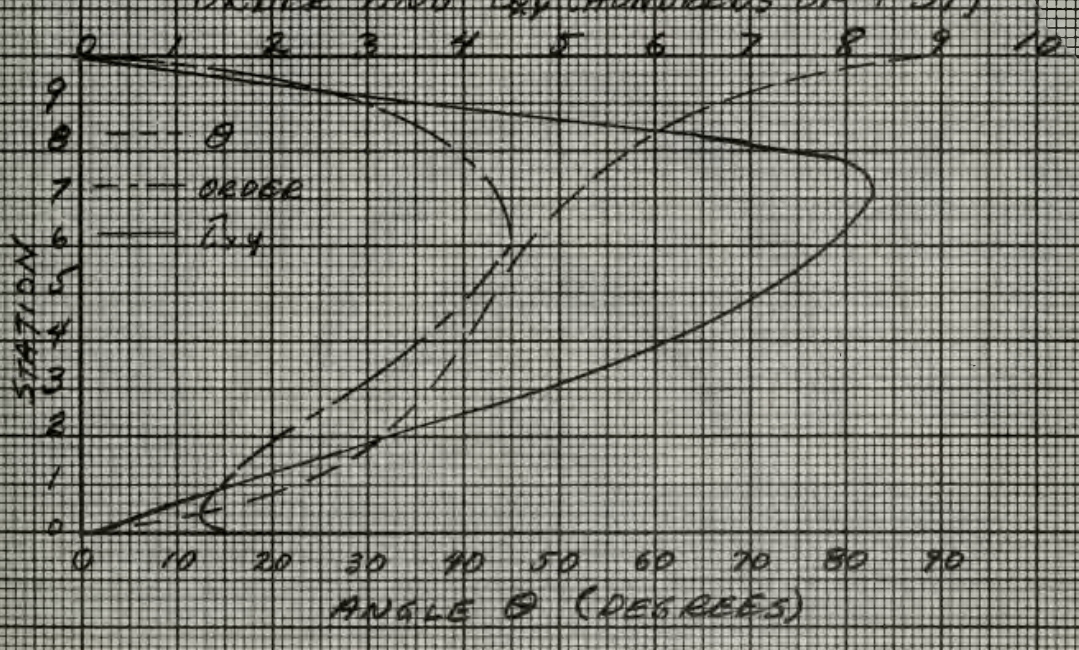
ORDER AND $\bar{\tau}_{xy}$ (HUNDREDS OF PSI)
0 1 2 3 4 5 6 7 8 9 10
θ
ORDER
$\bar{\tau}_{xy}$
STATION
0 1 2 3 4 5 6 7 8 9
0 10 20 30 40 50 60 70 80 90
ANGLE θ (DEGREES)

Figure XXVII

TABLE VI

Aspect Ratio 3:1 Plate Stiffened (1 stiffener)

Bottom Unsupported Load 500 psi

Station	Order	θ	2θ	Sin 2θ	τ_{xy}
0	1.4	0	0	0	0
1/2	1.4	14	28	.470	114
1	2.0	21	42	.669	231
2	3.3	29	58	.848	485
3	4.6	35	70	.940	750
4	5.2	40	80	.985	887
5	5.6	44	88	.994	965
6	5.1	49	98	.986	871
7	4.3	54	108	.950	707
8	3.1	62	124	.830	446
9	1.9	72	144	.588	194
9 1/2	1.4	79	158	.374	90.8
10	1.0	90	180	0	0

Bottom Supported Load 500 psi

Station	Order	θ	2θ	Sin 2θ	τ_{xy}
0	2.1	0	0	0	0
1/2	1.9	14	28	0.420	155
1	2.0	22	44	0.695	240
2	2.9	33	66	0.914	459
3	3.4	40	80	0.985	521
4	4.0	45	90	1.000	693
5	4.5	48	96	0.995	776
6	4.1	51	102	0.980	695
7	3.4	58	116	0.900	530
8	2.5	67	134	0.720	312
9	1.6	76	152	0.470	130
9 1/2	1.3	82	164	0.276	62.2
10	1.0	90	180	0	0

FIGURE XXVIII

ASPECT RATIO 3:1 STIFFENED & UNSUPPORTED

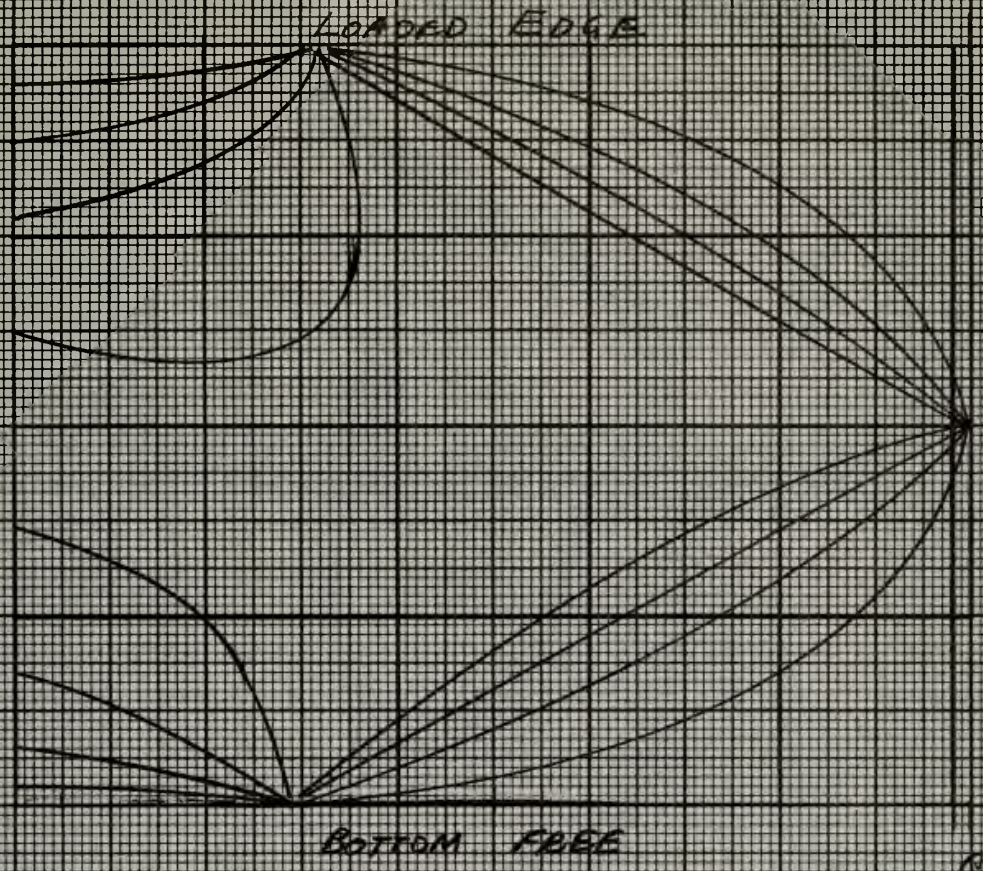

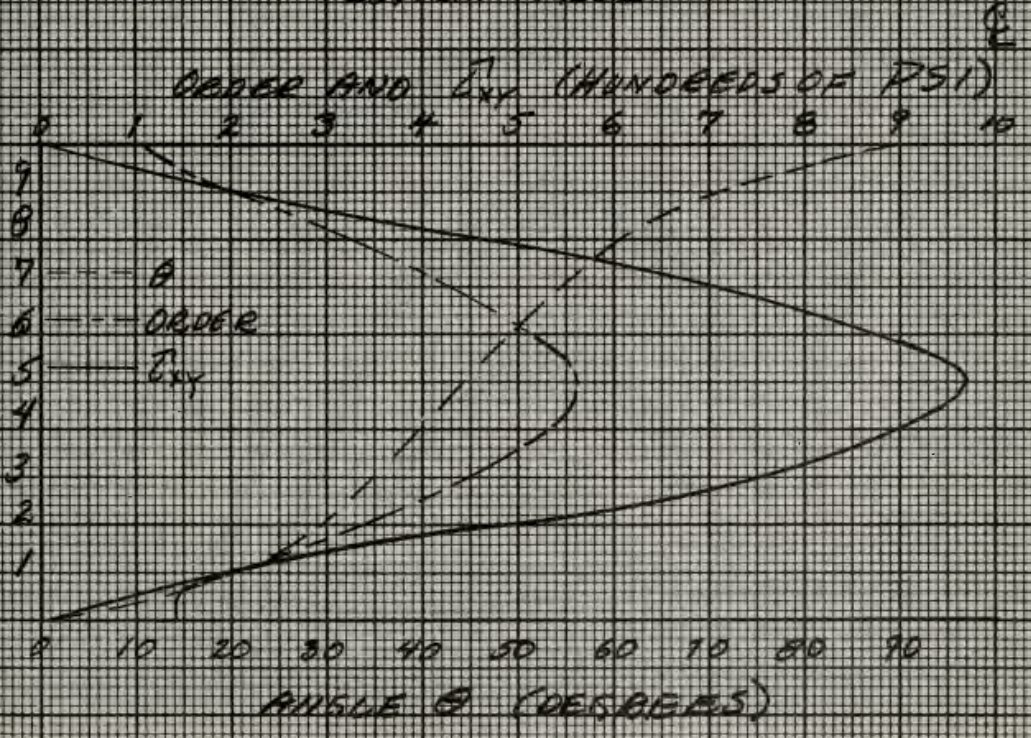
ORDER AND $\bar{\sigma}_{xy}$ (HUNDREDS OF PSI)
0 1 2 3 4 5 6 7 8 9 10
STATIONS
9 8 7 6 5 4 3 2 1
θ
ORDER
$\bar{\sigma}_{xy}$
0 10 20 30 40 50 60 70 80 90
ANGLE θ (DEGREES)

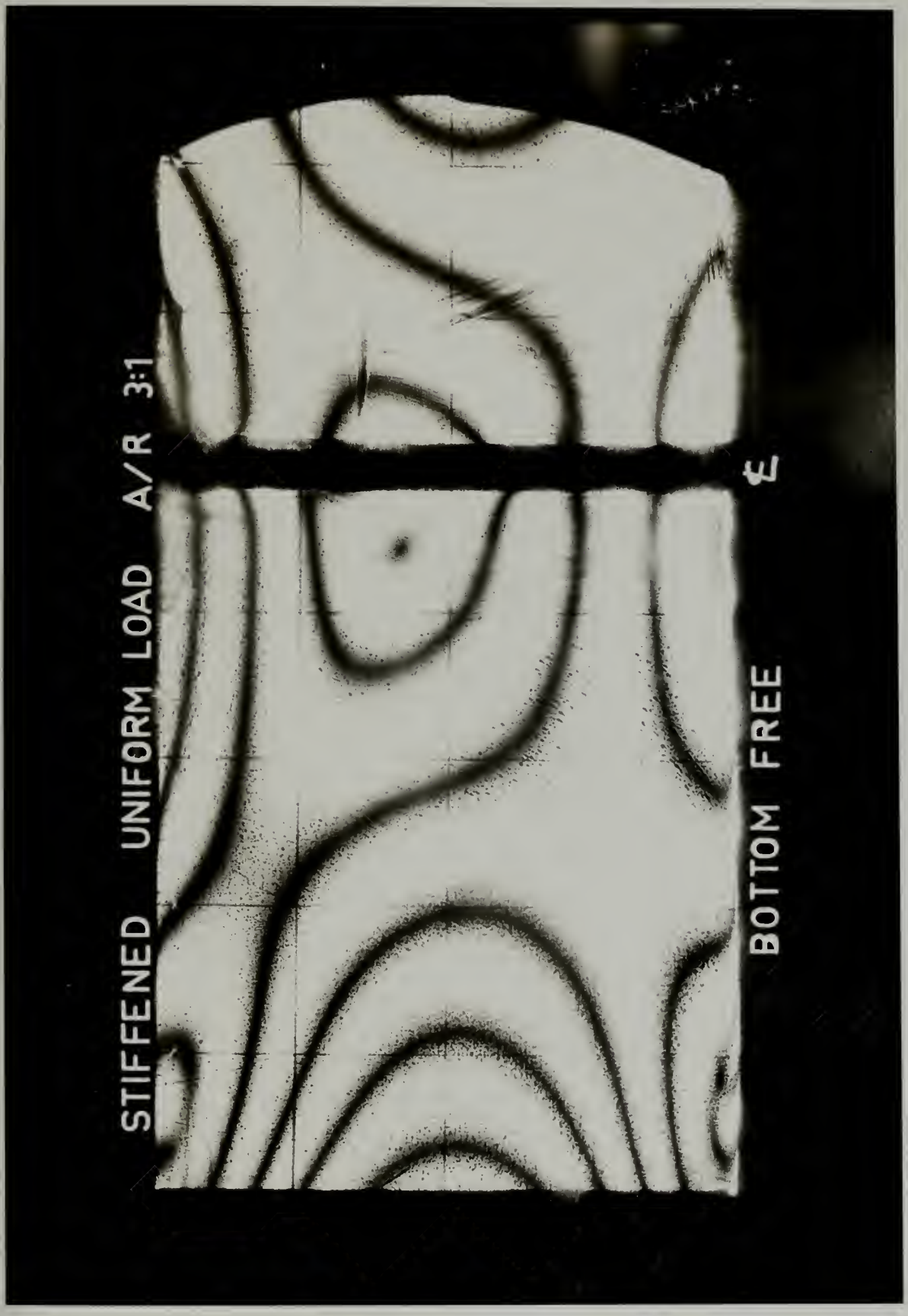

FIGURE XXIX

FIGURE XXX

ASPECT RATIO 3:1 STIFFENED & SUPPORTED

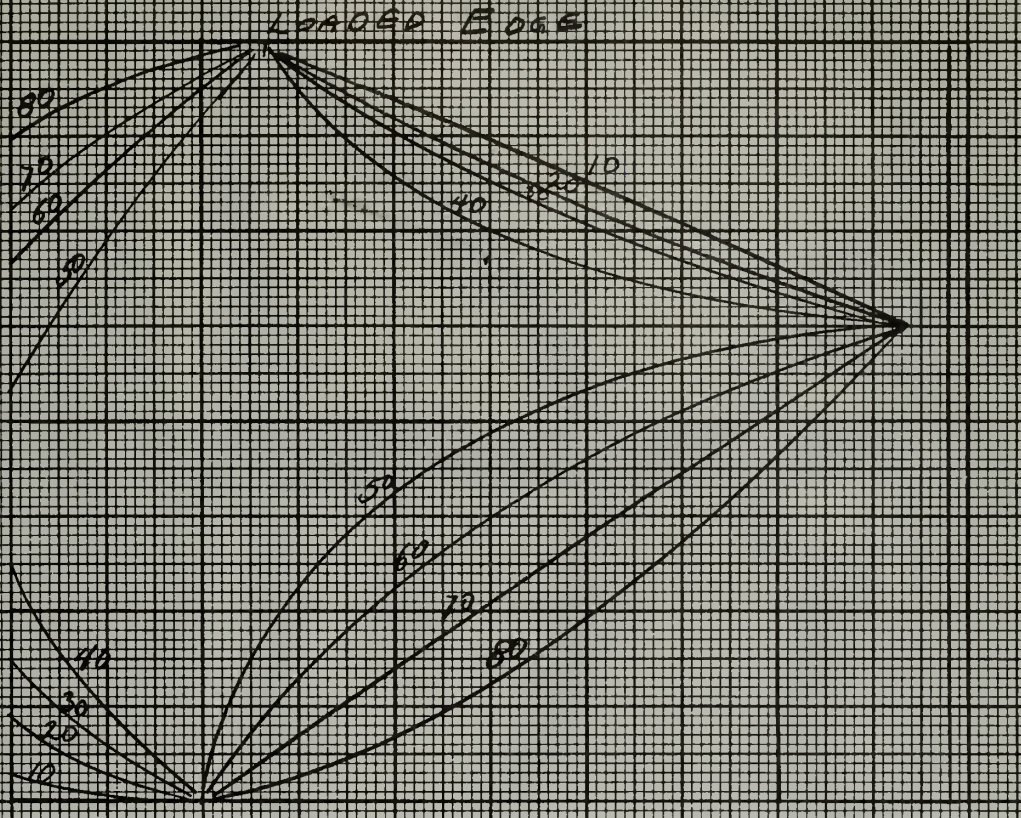

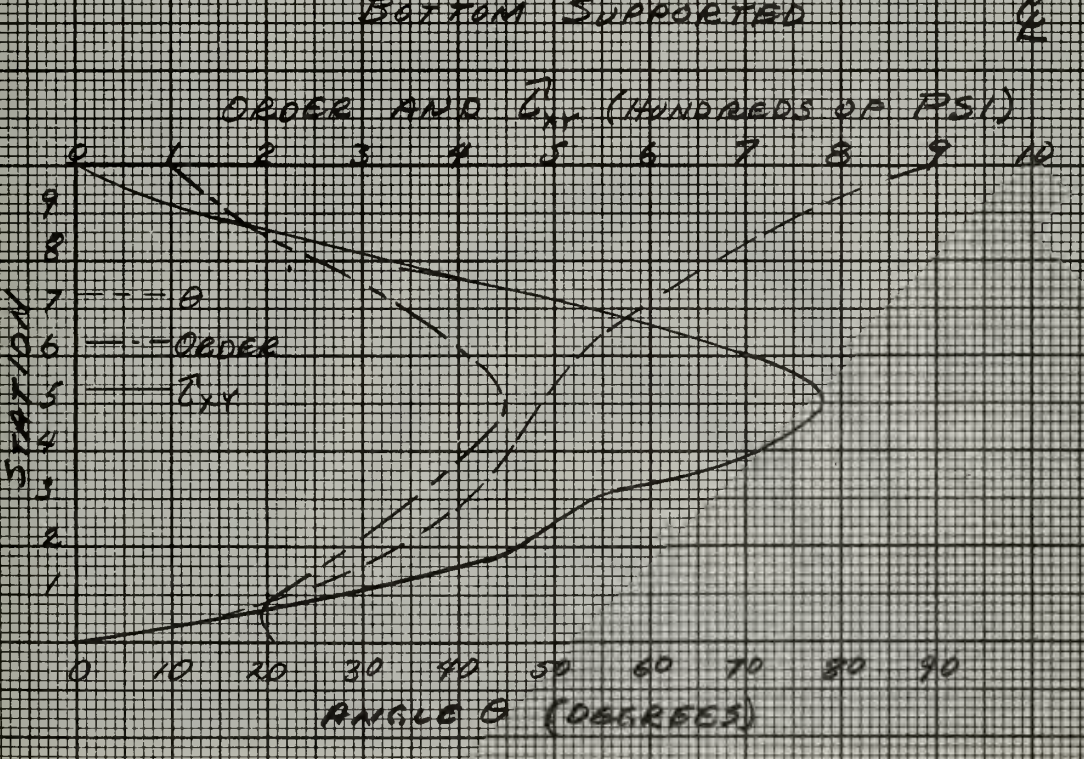

Figure XXXI

TABLE VII

Aspect Ratio 3:1 Plate Stiffened (3 stiffeners)

Bottom Unsupported Load 500 psi

Station	Order	θ	2θ	Sin 2θ	τ_{xy}
0	1.8	0	0	0	0
1/2	1.9	11	22	.376	123.4
1	2.1	20	40	.642	234
2	3.2	31	62	.883	490
3	4.4	36	72	.950	725
4	5.3	41	82	.988	913
5	6.0	44	88	.999	1040
6	6.2	47	94	.996	1070
7	6.0	52	104	.970	1005
8	5.1	60	120	.866	764
9	3.5	71	142	.615	372
9 1/2	2.8	80	160	.342	166
10	1.5	90	180	0	0

Bottom Supported Load 500 psi

Station	Order	θ	2θ	Sin 2θ	τ_{xy}
0	0.5	0	0	0	0
1/2	0.9	14	28	.469	73
1	1.2	26	52	.788	164
2	2.1	35	70	.940	342
3	2.9	38	76	.970	487
4	3.3	41	82	.988	565
5	3.8	45	90	1.000	658
6	4.0	48	96	.994	689
7	3.8	54	108	.950	626
8	3.0	60	120	.866	450
9	1.9	69	138	.669	220
9 1/2	1.5	79	158	.374	97.2
10	1.0	90	180	0	0

FIGURE XXXII

CASE 3.1 THREE STIFFENERS, UNASSOCIATED

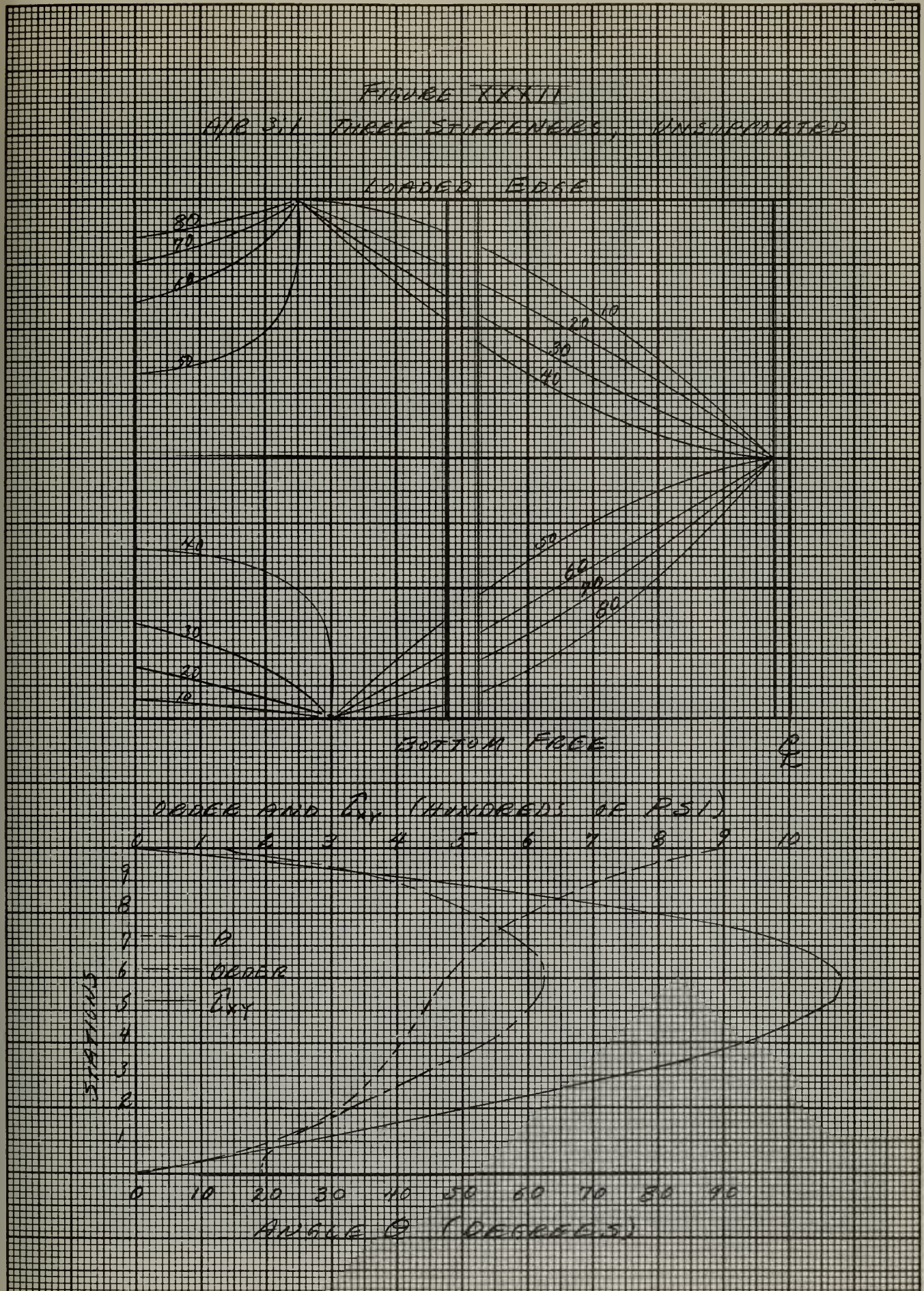

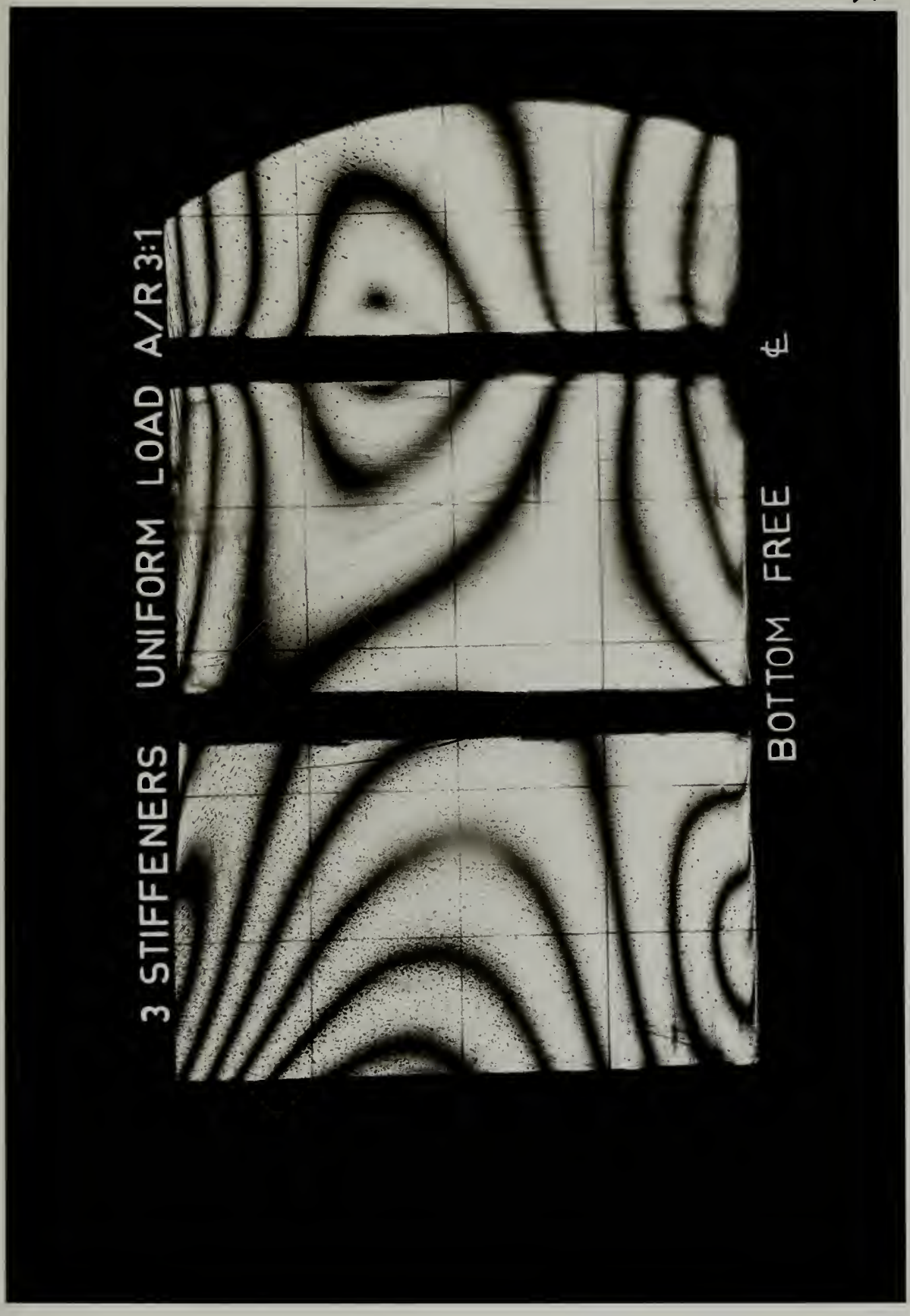

FIGURE XXXIII

FIGURE XXXIV

A/R 3:1 THREE STIFFENERS, SUPPORTED

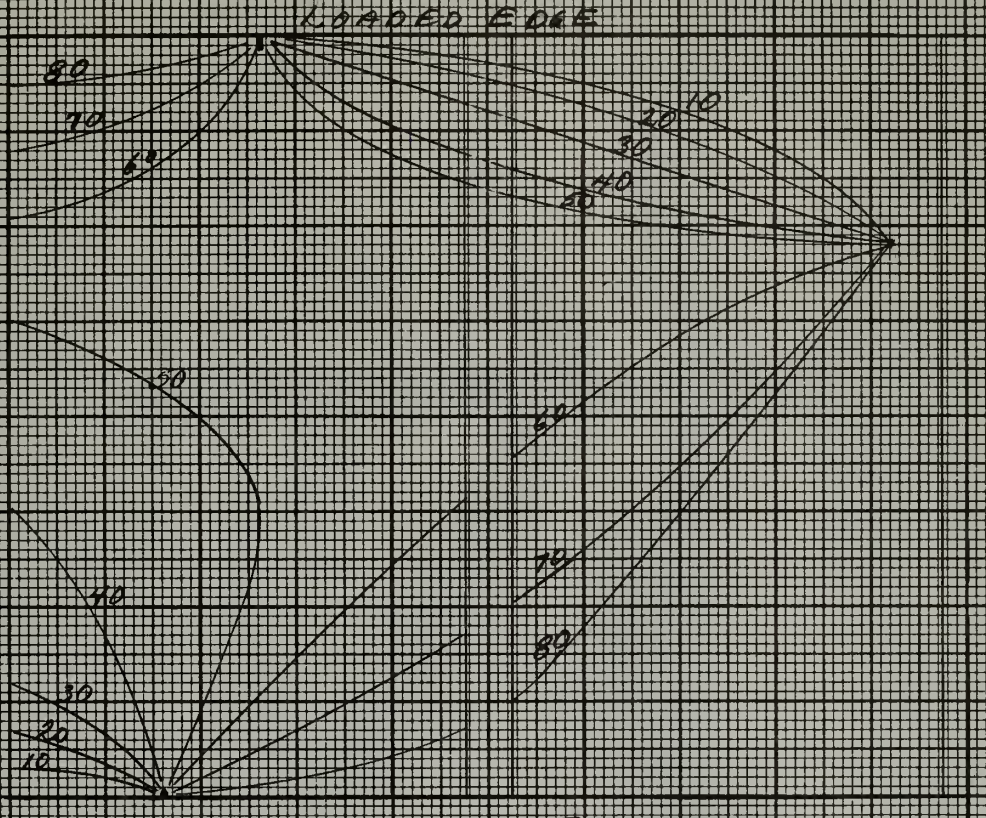

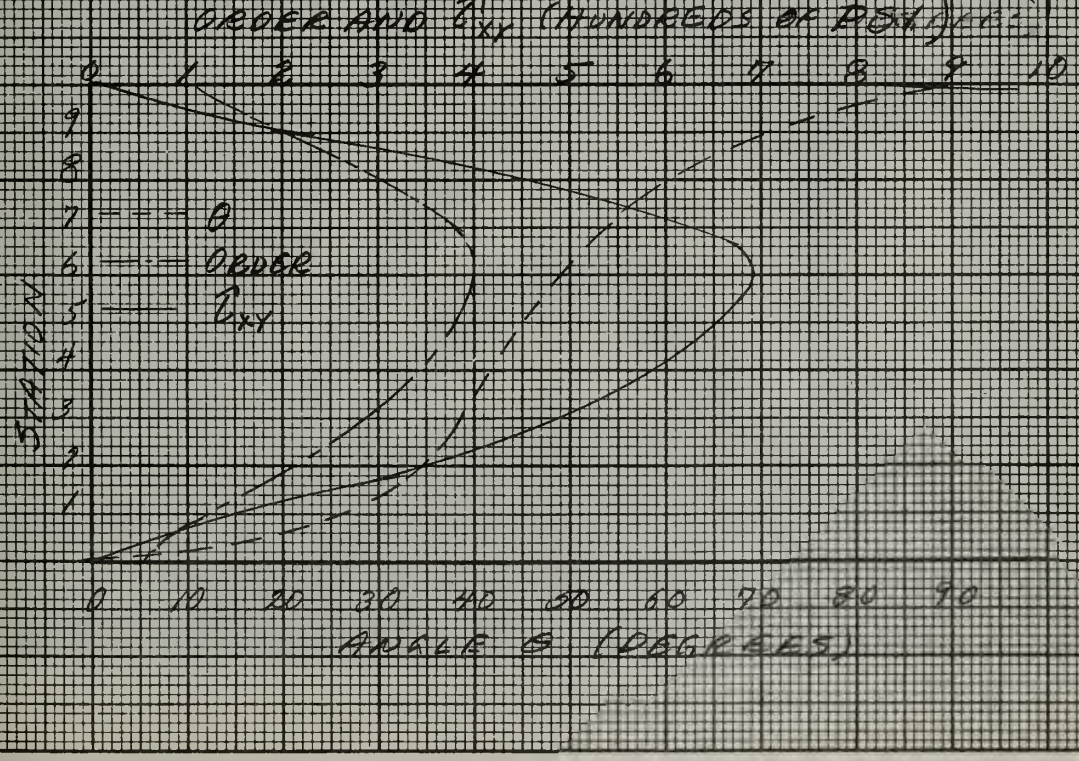

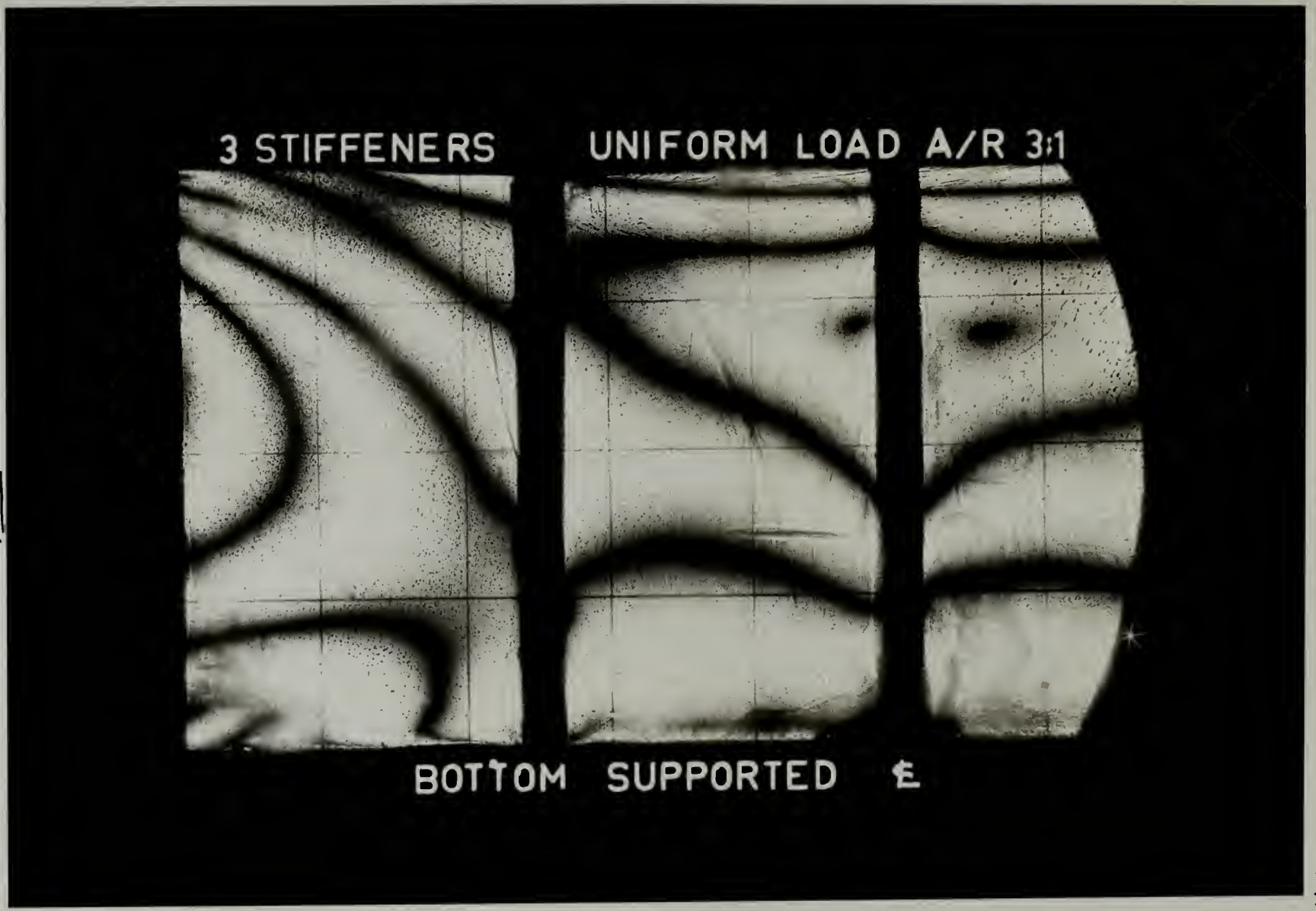

Figure XXXV

TABLE VIII

Aspect Ratio 2:1 Plate Unstiffened

Bottom Unsupported Load 500 psi

Station	Order	θ	2θ	Sin 2θ	τ_{xy}
0	0	90	180	0	0
1/2	0.5	63	126	.809	70.0
1	0.9	48	96	.994	155
2	1.7	21	42	.669	197
3	2.4	0	0	0	0
4	3.0	21	42	.669	347
5	3.4	33	66	.914	538
6	3.5	40	80	.985	597
7	3.3	47	94	.997	570
8	3.0	56	112	.927	482
9	1.9	70	140	.643	215
9 1/2	1.0	79	158	.375	65.0
10	0	90	180	0	0

Bottom Supported Load 500 psi

Station	Order	θ	2θ	Sin 2θ	τ_{xy}
0	0	0	0	0	0
1/2	1.0	8	16	.276	47.8
1	1.1	15	30	.500	95.2
2	1.5	28	59	.856	222
3	1.9	37	74	.960	316
4	2.2	42	82	.988	376
5	2.6	44	88	.999	451
6	3.0	45	90	1.000	520
7	3.3	48	96	.994	568
8	3.3	54	108	.950	543
9	2.8	67	134	.720	349
9 1/2	1.6	77	154	.433	120
10	0	90	180	0	0

FIGURE XXXVI

A/R 2:1 UNSTIFFENED & UNSUPPORTED

ORDER AND τ_{xy} (HUNDREDS OF PSI)

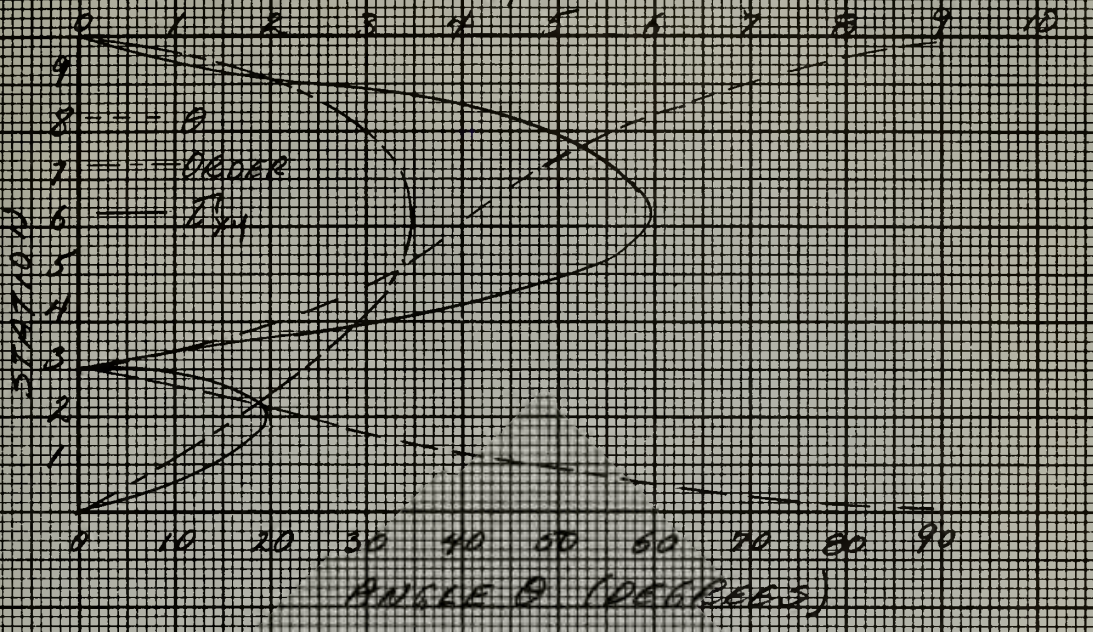

FIGURE XXXVII

A/R 2:1 UNSTIFFENED & SUPPORTED

ORDER AND τ_{xy} (HUNDREDS OF PSI)

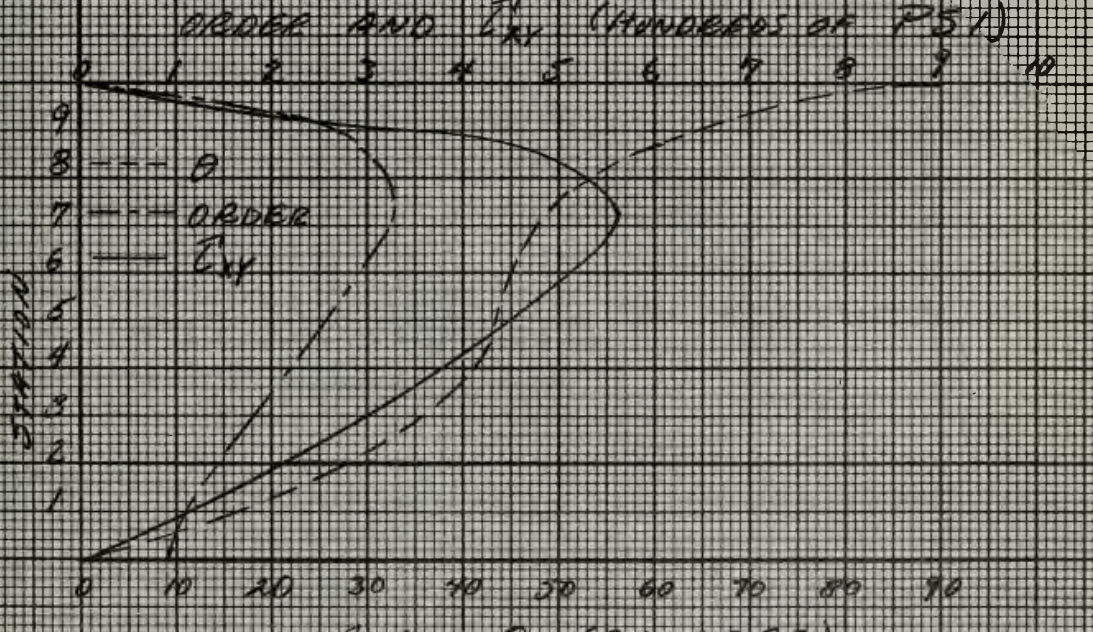

FIGURE XXXVII

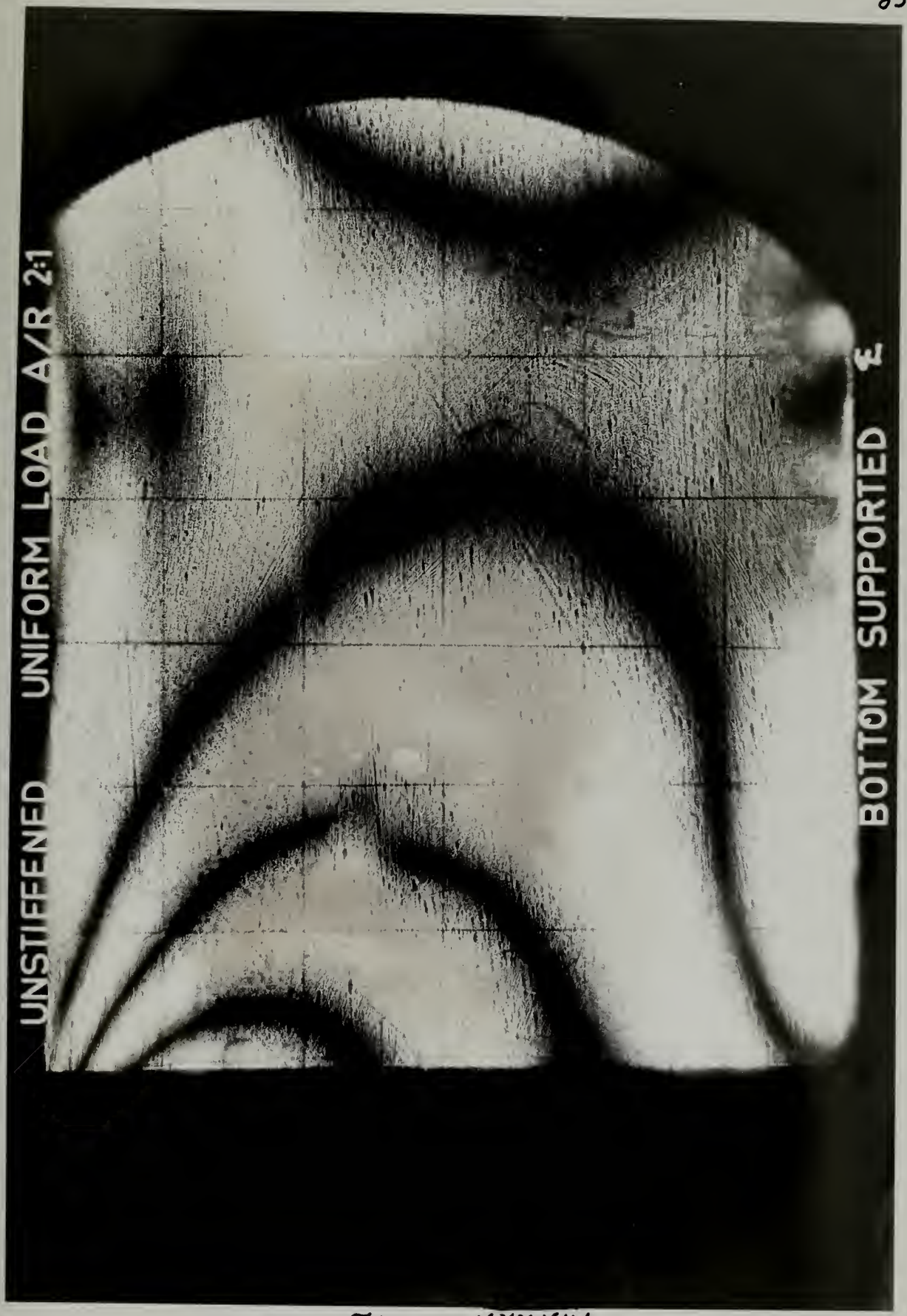

Figure XXXVIII

TABLE IX

Aspect Ratio 2:1

Plate Stiffened

Bottom Unsupported Load 500 psi

Station	Order	θ	2θ	Sin 2θ	τ_{xy}
0	0	0	0	0	0
1/2	0.3	10	20	.342	17.8
1	0.9	16	32	.530	82.6
2	1.7	25	50	.765	226
3	2.5	30	60	.866	375
4	3.1	33	66	.914	490
5	3.5	36	72	.950	576
6	3.9	41	82	.986	667
7	3.9	48	96	.992	620
8	3.3	56	112	.927	529
9	2.1	69	138	.669	243
9 1/2	1.4	79	158	.374	90.8
10	0.5	90	180	0	0

Bottom Supported Load 500 psi

Station	Order	θ	2θ	Sin 2θ	τ_{xy}
0	0	53	106	.960	0
1/2	0.2	51	102	.978	33.9
1	0.4	49	98	.986	68.4
2	0.8	46	92	.999	139
3	1.4	43	86	.998	242
4	2.1	42	84	.994	362
5	2.5	41	82	.986	427
6	2.9	44	88	.999	502
7	3.1	50	100	.985	529
8	3.1	57	114	.914	490
9	2.3	66	132	.744	296
9 1/2	1.7	77	154	.438	129
10	0	90	180	0	0

Figure XXXIII

A/R 2:1 STIFFENED & UNSUPPORTED

Order & τ_{xy} (Hundreds of psi)

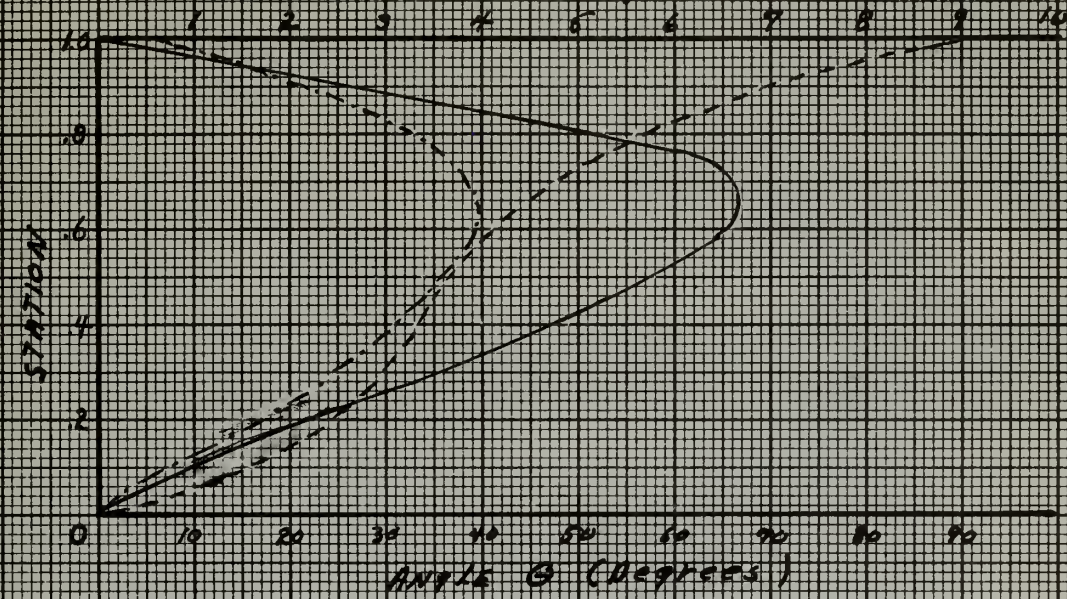

Figure XXXIV

A/R 2:1 STIFFENED & SUPPORTED

ORDER & τ_{xy} (Hundreds of psi)

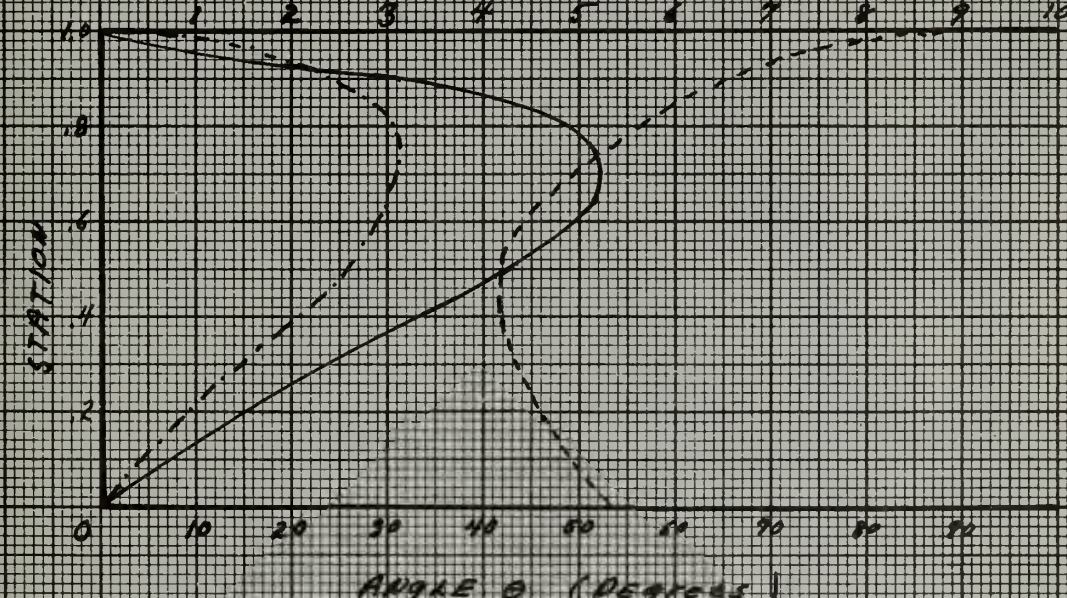

STIFFENED
BOTTOM FREE

Figure XLIII

APPENDIX E

Literature Citations

(1) Holman, R. — "A Photoelastic Study of the Stress Distribution in Stiffened Plating" Thesis – Dept. of Naval Arch. and Marine Eng. - M.I.T., 1956

(2) Figueiredo, A.R., Marangiello, D.A., and Guerra, W. V. — "A Photoelastic Study of the Stress Distribution in Ship Transverse Bulkheads" - Thesis - Dept. of Naval Arch. and Marine Eng. - M.I.T., 1956.

(3) Freire, T. D., DaSilva Sa, J.B., Serraro, R.O. — "A Photo-Elastic Study of the Stress Distribution in Flat Plating Panels" Thesis - Dept. of Naval Arch. and Marine Eng. - M.I.T., 1956.

(4) Durelli, A.J., Lake, R.L. and Tsao, C.H. — "Device for Applying Uniform Loading to Boundaries of Complicated Shape" - The Proceedings of the Society for Experimental Stress Analysis (hereafter SESA) Vol I-I

(5) Frocht, M.M. — "Photo-Elasticity," Vol. I, New York: John Wiley and Sons, 1941.

(6) Frocht, M.M. — "Photo-Elasticity," Vol. II, New York, John Wiley and Sons, 1948.

(7) Hendry, A. W. — "The Stress Distribution in a Simply Supported Beam of I-Section carrying a Central Concentrated Load" - AESA - 1950.

(8) Chou, Li, Conway, H.D., and Winter, G. — "Stress in Deep Beams" - Trans. of the American Society of Civil Engineers - 1953.

(9) Becker, H. — "Photoelastic analysis of a Spar Bulkhead in a Semi- Monocoque Airplane Fuselage" - SESA -Vol.IV-I.

(10) Paffett, J. A. H. — "The Application of Photoelastic Methods to Ship Design Problems" Trans. of the North-East Coast Institution of Engineers and Ship-Builders, 1950.

(11) Coker, E. G. "The Determination by Photo-elastic Methods, of the Distribution of Stress in Plates of Variable Section with Some Application to Ship Plating" Transactions of the Institute of Naval Architects, 1911.

JA 17 58 BINDERY

Thesis 35899
M5859 Miller
A photoelastic study of the stress distribution in flat plate panels simulating ship bulkheads.
JA 17 58 BINDERY

Thesis 35899
M5859 Miller
A photoelastic study of the stress distribution in flat plate panels simulating ship bulkheads.

thesM5859
An photoelastic study of the stress dist
3 2768 001 88375 4
DUDLEY KNOX LIBRARY